Marine Pollution Bulletin
December 2022, Volume 185 Pages 114315 (11p.)
https://doi.org/10.1016/j.marpolbul.2022.114315
https://archimer.ifremer.fr/doc/00804/91584/

Isotopic compositions of copper and zinc in plankton from the Mediterranean Sea (MERITE-HIPPOCAMPE campaign): Tracing trophic transfer and geogenic inputs

Chifflet Sandrine [1, *], Briant Nicolas [2], Freydier Rémi [3], Ferreira Araujo Daniel [2], Quéméneur Marianne [1], Zouch Hana [4], Bellaaj-Zouari Amel [4], Carlotti François [1], Tedetti Marc [1]

[1] Aix Marseille Univ., Université de Toulon, CNRS, IRD, MIO UM 110, 13288 Marseille, France
[2] Ifremer, CCEM Contamination Chimique des Écosystèmes Marins, F-44000 Nantes, France
[3] HSM, Université de Montpellier, CNRS, Montpellier, France
[4] Institut National des Sciences et Technologies de la Mer (INSTM), 28, rue 2 mars 1934, Salammbô 2025, Tunisia

* Corresponding author : Sandrine Chifflet, email address : sandrine.chifflet@mio.osupytheas.fr

Abstract :

This study uses Cu and Zn isotopic compositions as proxies of sources and metal transfers in the planktonic food webs from the Mediterranean Sea. Plankton was collected in spring 2019 in the deep chlorophyll maximum (DCM) along a North-South transect including coastal and offshore zones (MERITE-HIPPOCAMPE campaign). δ65Cu and δ66Zn were determined on four planktonic size fractions from 60 to 2000 µm. Combined δ65Cu and δ66Zn with geochemical tracers (Ti, particulate organic phosphorus) showed that geogenic particles were ubiquitous with plankton assemblages. The δ15N ecological tracer showed that planktonic food web was enriched in heavy isotopes of Cu and Zn in the higher trophic levels. δ65Cu were correlated with picoplankton in the offshore zone, and with zooplankton in the southern coastal zone. Firmicutes bacteria were found correlated with δ66Zn in northern and southern coastal zones suggesting decomposition of particulate matter at the DCM. These findings suggest that biogeochemical process may impact Cu and Zn isotopy in the planktonic community.

Highlights

► Cu and Zn transfers in the Mediterranean planktonic food web ► $\delta^{65}Cu$ and $\delta^{66}Zn$ compositions are impacted by geogenic inputs. ► $\delta^{65}Cu$ and $\delta^{66}Zn$ compositions correlated with planktonic community.

Keywords : Mediterranean Sea, Planktonic food webs, Cu and Zn isotopes, Geogenic inputs

1. Introduction

Plankton is an important gateway for the accumulation and transfer of trace metal into the marine food web (Rossi and Jamet, 2008; Chouvelon et al., 2019). According to their role in biogeochemical cycles, copper (Cu) and zinc (Zn) can be categorized as essential for marine food web. Indeed, both elements serve as co-factors in enzymes of key metabolic pathways. Cu is a key micronutrient that contributes to photosynthesis, denitrification and iron uptake by primary producers in the food web (Peers et al., 2005; Peers and Price, 2006; Zumft and Kroneck, 2007). However, above 10 pM, free dissolved copper (Cu^{2+}) exerts acute toxic effects on phytoplankton (Moffett et al., 1997) which in turn may release organic ligands that strongly complex Cu as an effective detoxification mechanism (Moffett and Brand, 1996; Croot et al., 2000; Rue and Bruland, 2001). Zn containing enzymes are carbonic anhydrases, essential during biomass buildup from reduced carbon and light (Domsic et al., 2008), or alkaline phosphatases for the acquisition of organic phosphorus when phosphate is scarce (Morel and Price, 2003; Shaked et al., 2006; Cox and Saito, 2013). Because the interactions between metal and organisms are numerous and complex, it is still difficult to understand transfers of Cu and Zn in the planktonic food web.

The new generation of high-resolution mass spectrometers, such as the multi-collector inductively coupled plasma mass spectrometers (MC-ICP-MS), have allowed measuring accurately isotope compositions of trace metal in natural marine samples (Araújo et al., 2022a). Cu has two stable isotopes, ^{63}Cu and ^{65}Cu, with natural average abundances of 69.17 and 30.83%, respectively, while Zn has five stable isotopes, ^{64}Zn, ^{66}Zn, ^{67}Zn, ^{68}Zn, and ^{70}Zn, with natural average abundances of 48.63, 27.90, 4.10, 18.75, and 0.62%, respectively (Maréchal et al., 1999). In natural ecosystems, the relative abundance of stable isotopes varies according to isotopic fractionation phenomena occurring during biogeochemical processes, between reactants and products, phases or molecules (Wiederhold, 2015). These changes in isotope

ratios have proven useful in tracing sources and biogeochemical processes in hydrothermal systems (Larson et al., 2003; Rouxel et al., 2004; Maher and Larson, 2007), ore deposits (Graham et al., 2004; Mason et al., 2005; Lemaitre et al., 2020a) and open ocean (Conway and John, 2014; Conway et al., 2021). In coastal marine ecosystems, these isotopes have been relevant to track metal dispersion and to differentiate the type and nature of particles (natural *versus* anthropogenic, mineral *versus* organic) by river inputs or atmospheric deposition (Araújo et al., 2022a; b).

However, the Cu and Zn isotopic fractionation related to planktonic organisms, colloids and the dissolved matrix in seawater is not yet clearly elucidated. Cu speciation is dominated by Cu^{2+} complexation with organic ligands (Coale and Bruland, 1988; Moffett et al., 1990) and induces a significant isotopic fractionation ($\Delta^{65}Cu_{complex\text{-}free}$ ranging from +0.1 to +0.8‰) during equilibrium exchanges between organically complexed and free inorganic dissolved Cu (Bigalke et al., 2010; Fujii et al., 2013; Ryan et al., 2014). Zn bound to organic ligands exhibits an isotopic fractionation ($\Delta^{66}Zn_{cell\text{-}sw}$) ranging from -0.8 to -0.2‰ depending on homeostasis pathways during phytoplankton photosynthesis (John et al., 2007a; Peel et al., 2009; John and Conway, 2014). While many studies have investigated the magnitude of Cu and Zn isotopic fractionations under controlled laboratory conditions, few field studies applied these insights to constrain the transfer mechanisms of the elements in real environmental conditions.

The Mediterranean Sea is a semi-enclosed sea that covers ~ 0.7% of the total ocean surface area (~ 0.25% by volume), contains 4 to 18% of the world's marine diversity (Bianchi and Morri, 2000; UNEP/MAP-RAC-SPA, 2008) and is characterized by oligotrophic conditions due to its low content in nutrient (The Mermex group, 2011; Marañón et al., 2021). The Mediterranean Sea is subject to natural and anthropogenic exogenous chemical substances coming from rivers, effluents and atmospheric deposition (Guieu et al., 2002; Heimbürger et al., 2010, 2011; Pey et al., 2010; Llamas-Dios et al., 2021; Desboeufs et al., 2022). Important

changes have been observed in recent decades in small pelagic fish populations of the northwestern Mediterranean Sea related to various environmental factors (Coll et al., 2019). Multiple drivers including climatic (temperature, UV irradiance), acidification, demersal fishing, ship traffic and coastal pollution would affect 20% of the entire basin and 60–99% of the territorial waters of EU member states of the Mediterranean and Black Seas (Micheli et al., 2013). Among the pollutants, trace metals are a recurrent concern (Luy et al., 2012).

In order to further understand the biogeochemical cycles of Cu and Zn in the Mediterranean Sea, isotopic compositions of these elements were determined within the planktonic food web (from bacteria to zooplankton) according to three Mediterranean geographical areas: the northern and southern coastal zones, and the offshore zone. Based on these geographical areas, we aim thus to identify geogenic (natural and anthropogenic mineral sources) and biological (planktonic sources) fingerprints and to evidence their underlying biogeochemical processes. The abundance, diversity and taxonomy of plankton assemblages (bacterio-, phyto-, and zoo-plankton) are presented as companion papers (Quéméneur et al., 2022; Bellaaj Zouari et al., 2022; Fierro-González et al., 2022) and are used in this study to support the discussion.

2. Materials and methods

2.1. Study zone and sampling procedure

The MERITE-HIPPOCAMPE campaign was conducted on the R/V *Antea* (Tedetti and Tronczynski, 2019) in spring 2019 along a north-south Mediterranean transect, between the French (Toulon and Marseille, northwestern Mediterranean Sea) and Tunisian coastal zones (Gulf of Gabès, southeastern Mediterranean Sea) according to two legs and ten sampling stations (Table 1). Leg 1 was carried out between April 13th and 28th with sampling of 5 stations

(St2, St4, St3, St10 and St11; in this chronological order) during the transect from La Seyne-sur-mer to Tunis. Leg 2 was carried out between April 30th and May 14th with sampling of 5 stations (St19, St17, St15, St9, St1; in this chronological order) during the return transect from the Gulf of Gabès to La Seyne-sur-mer (Fig. 1; Table 1). Sampling strategy implied a wide spatio-temporal variability between stations. They were chosen according to different criteria of physical, biogeochemical and biological conditions (Tedetti et al., 2022). We divided the transect in three geographical areas: i) the northern coastal zone (St1 to St4), located in the bays of Toulon and Marseille, ii) the southern coastal zone (St15, St17 and St19), located along the Tunisian coasts and iii) the offshore zone (St9 to St11), located in near the northern zone of the Balearic Thermal Front (St9 and St10), and in the Algerian ecoregion (St11).

At each station, a Multiple Horizontal Plankton Sampler (Midi type, Hydro-Bios®), referred to hereafter as "MultiNet", was deployed to collect horizontally plankton in the deep chlorophyll maximum (DCM; Table 1). In a clean lab-container, recovered plankton was fractionated into four size fractions (F3: 60–200 µm, F4: 200–500 µm, F5: 500–1000 µm and F6: 1000–2000 µm) using nylon sieves by wet-sieving with seawater previously filtered through a glass fibre filter (GF/F, Whatman®). The four plankton size fractions were partitioned for various analyses (Tedetti et al., 2022) and aliquots for trace metal and isotopic analysis were transferred into pre-cleaned (HCl, 10%) polycarbonate jars and stored at -20 °C.

2.2. Analytical procedures

2.2.1. Elemental concentrations

The sample processing was carried out in a trace metal clean laboratory (ISO 5), using high purity acids (Optima grade, Fisher), and ultrapure water (Milli-Q® EQ 7000, Millipore). Planktonic samples (~200 mg dw) were digested in PFA vials (Savillex) with 5 mL of a mixture of pure acids (HF, 0.5 mL; HNO_3, 4.5 mL), heated on a hot-block (120 °C, 24 h), evaporated

to near dryness, and re-dissolved in 3 mL of HNO_3 (10%). The digested samples were then diluted using HNO_3 (2%) before running the trace metal analyses. Elemental analyses were performed by an inductively-coupled plasma mass spectrometer (ICP-MS; ICAP-Q™; ThermoScientific®) at the Laboratoire de Biogéochimie des Contaminants Métalliques (LBCM, Ifremer, Nantes). Details of laboratory and analytical procedures concerning trace metal analyses were described in a companion paper (Chifflet et al., 2022).

2.2.2. Chromatographic separation

Prior to isotopic analyses, Cu and Zn were separated from the digested samples by ion exchange chromatography according to the following modified protocol (Borrok et al., 2007). All critical laboratory equipment (PFA vials, micropipette tips, columns and PFA storage bottles) were acid cleaned before use. Separations were performed under a free-metal laminar flow hood installed in the clean laboratory (ISO 5). Aliquots of digested samples containing ~ 1000 ng of Cu were evaporated in PFA vials and re-dissolved in 1 mL HCl (10 M). Columns were loaded with 2 mL of pre-cleaned AG-MP1 anion exchange resin (100–200 mesh, Bio-Rad®), rinsed with 10 mL H_2O and conditioned with 10 mL HCl (10 M). Samples were loaded onto the columns and rinsed with 5 mL HCl (10 M) to elute the matrix. Then, Cu fractions were eluted with 20 mL HCl (5 M) followed by Zn fractions with 15 mL HCl (0.01 M). All steps were repeated 3 times to complete purification of Cu and Zn. The analyte content recoveries (100 ± 10%) and presence of interfering elements (Ba, Ca, Cr, Mg, Na, Ni, Ti, V) in Cu and Zn fractions were checked by ICP-MS (ICAP-Q™; ThermoScientific) to assure no bias effect on isotope measurements (Maréchal and Albarède, 2002; Petit et al., 2008; Schleicher et al., 2020). Procedural blanks were below 1% of Zn and Cu mass contents in fractions. After purification, Cu and Zn fractions were near-dried and re-dissolved in HNO_3 for isotope ratio measurements.

2.2.3. Isotopic analysis

Cu and Zn isotopic compositions were measured by MC-ICP-MS (Neptune Plus™; ThermoScientific) in low mass resolution mode using a SIS (Stable Introduction System) nebulization chamber and a low flow PFA self-aspiration nebulizer. Cu isotopes (^{63}Cu, ^{65}Cu) were measured at the PSO platform (Ifremer, Brest). Cu fractions were dissolved at 250 µg/L in HNO_3 (2%, v/v) and introduced at 50 µL/min. Zinc isotopes (^{64}Zn, ^{66}Zn, ^{67}Zn, ^{68}Zn) were measured at the AETE-ISO platform (OSU-OREME university, Montpellier). Zn fractions were dissolved at 250 µg/L in HNO_3 (1%, v/v) and introduced at 70 µL/min. Zinc isotopes (^{64}Zn, ^{66}Zn, ^{67}Zn, ^{68}Zn), Cu isotopes (^{63}Cu, ^{65}Cu) and Ni isotope (^{62}Ni) were monitored simultaneously and ^{62}Ni was used to correct possible isobaric ^{64}Ni interferences on ^{64}Zn.

Instrumental mass fractionation was corrected as described by Bermin et al. (2006) and Zhao et al. (2014). For the Cu isotope analyses, a Zn internal standard (Zn_{ETH}) was added to the purified Cu fractions and a mixture of external standards (Cu_{SRM976} + Zn_{ETH}) was run with a standard bracketing sequence. The mass bias correction on the ^{65}Cu/^{63}Cu ratio was performed combing the internal and external normalization using Zn isotopes ratios (^{66}Zn/^{64}Zn, ^{67}Zn/^{64}Zn, ^{68}Zn/^{64}Zn, and ^{68}Zn/^{66}Zn) and an exponential law correction. The final Cu isotopic compositions (δ^{65}Cu) were reported relative to NIST SRM976 as follow (Eq.1):

$$\delta^{65}Cu_{SRM976}(‰) = \left(\frac{\left(\frac{^{65}Cu}{^{63}Cu}\right)_{sample}}{\left(\frac{^{65}Cu}{^{63}Cu}\right)_{SRM\ 976}} - 1 \right) \times 1000 \qquad \text{(Eq. 1)}$$

For the Zn isotope analyses, a Cu internal standard (Cu_{SRM976}) was added to the purified Zn fractions and the mixture of external standards (Cu_{SRM976} + Zn_{ETH}) was unchanged. Due to the depletion of the Zn standard ($Zn_{JMC\text{-}Lyon}$), we replaced this latter by a new reference standard (Zn_{ETH}). However, we chose to express our δ^{66}Zn values relative to JMC-Lyon in order to compare our data with the literature (Araújo et al., 2017). Therefore, the $\delta^{66}Zn_{ETH}$ values were converted to $\delta^{66}Zn_{JMC\text{-}Lyon}$ values by adding a factor of 0.28‰ as recommended by Archer et

al. (2017). The final Zn isotopic compositions (δ^{66}Zn) relative to JMC-Lyon were expressed as follow (Eq. 2):

$$\delta^{66}Zn_{JMC-Lyon}(‰) = \left(\frac{\left(\frac{^{66}Zn}{^{64}Zn}\right)_{sample}}{\left(\frac{^{66}Zn}{^{64}Zn}\right)_{ETH}} - 1 \right) \times 1000 + 0.28 \qquad \text{(Eq. 2)}$$

External precision (2σ) was obtained from repeated (2 to 3) measurements of samples. Long-term precision was assessed from plankton certified materials (BCR 414). The $\delta^{65}Cu_{BCr414}$ (-0.13 ± 0.12‰; n=2) agreed with reported values in literature (-0.29 ± 0.10‰; Yang et al., 2020; -0.27 ± 0.05‰; Takano et al., 2020). The $\delta^{66}Zn_{BCr414}$ (+0.42 ± 0.04‰; n=2) fell in the same range of published recommended value (+0.36 ± 0.10‰; Druce et al., 2020) and agreed with reported values in literature (+0.42 ± 0.04‰; Maréchal et al., 2002).

2.2.4. Isotopic analysis

Freeze-dried samples were ground to fine powder with an agate mortar and pestle. Approximately 0.5 mg of powder was weighed into a tin cup (8 × 5 mm) using a precision balance (d = 0.00001 g). N isotopic compositions were measured using elemental analyzer mass spectrometer Integra CN Sercon (Raimbault et al., 2008; Lacoste et al., 2016). N isotopes (^{14}N, ^{15}N) were carried out at the PACEM platform (Mediterranean Institute of Oceanography, Marseilles). The δ^{15}N composition was reported relative to conventional standard (atmospheric N_2) as follow (Eq. 3):

$$\delta^{15}N_{N2}(‰) = \left(\frac{\left(\frac{^{15}N}{^{14}N}\right)_{sample}}{\left(\frac{^{15}N}{^{14}N}\right)_{N2}} - 1 \right) \times 1000 \qquad \text{(Eq. 3)}$$

External precision (0.5 ‰) was obtained from repeated (2 to 3) measurements of samples.

2.3. Data processing

2.3.1. Biotic trace metal concentration

Marine particles are composed of complex assemblages of biotic (e.g., organic matter from living and dead organisms) and geogenic (e.g., minerals from natural and anthropogenic sources) components (Jeandel et al., 2015; Lam et al., 2018). The relative contribution of the latter component depends on the proximity and intensity of sources. In the field, the separation between biotic and geogenic particles remains an operationally challenging and requires an ultra-clean environment and specific equipment to avoid contaminations (Cullen and Sherrell, 1999; Plaquette and Sherrell, 2012).

However, using normalized ratios of particulate organic phosphorus (P-normalization), a biotic component equated to the fraction of organic matter can be estimated in marine particles (Ho et al., 2007; Liao et al., 2017).

$$[M]_{sample} = b.[POP]_b + a.[Ti]_a \quad \text{(Eq. 4)}$$

$$\frac{[M]_{sample}}{[Ti]_{sample}} \equiv b.\frac{[POP]_{sample}}{[Ti]_{sample}} + a \quad \text{(Eq. 5)}$$

where a is Ti-normalized elemental ratio in the geogenic component, b is P-normalized elemental ratio in the biotic component, $[M]_{sample}$ is elemental concentration in the sample, $[Ti]_a$ is Ti concentration in the geogenic component, and $[POP]_b$ is concentration of particulate organic phosphorus in the biotic component. Assuming that POP and Ti in samples are mainly due to the biotic and geogenic components, respectively ($[POP]_{sample} \equiv [POP]_b$; $[Ti]_{sample} \equiv [Ti]_a$), we can turn the mass balance formula into a first-order equation (Eq. 5) and resolved the model.

This technique has been extensively detailed by Chifflet et al. (2022) as companion paper and results (biotic, %) are summarized in Table 2.

2.3.2. Statistical analyses

Spearman correlation analyses were performed to identify relations between environmental variables using Xlstat software package version 2019.1.1 (Addinsoft 2020, Boston, USA, https://www.xlstat.com). A principal component analysis (PCA) was carried out to extract the key biological factors driving Cu and Zn isotopic composition based on the Spearman correlation test, with a statistical significance level higher than 95% ($p < 0.05$). It was performed using the abundance of bacterial, phytoplanktonic and zooplanktonic communities identified in samples and associated Cu, Zn isotope compositions.

3. Results and discussion

3.1. Cu and Zn isotopic composition in plankton

In the present study, isotopic compositions (δ^{65}Cu and δ^{66}Zn) in samples are explored in relation to their respective concentrations (Cu and Zn) in four particles size fractions (F3: 60–200 µm, F4: 200–500 µm, F5: 500–1000 µm and F6: 1000–2000 µm) collected into the DCM in order to better understand the biogeochemical cycles of Cu and Zn within the Mediterranean planktonic food web (Fig. 2; Table 3). Note that some samples (*i.e.*, St1-F3 and St1-F6) had too little amount of Cu and Zn (< 1000 ng) to perform isotopic analysis, which explains some missing data in Table 3. All other data of the MERITE-HIPPOCAMPE campaign for trace metal (As, Cd, Cr, Cu, Fe, Mn, Ni, Sb, Ti, V, Zn) and associated particulate organic phosphorus (POP) in the four size fractions are detailed in a companion paper (Chifflet et al., 2022).

The Cu isotopic composition (δ^{65}Cu) in the different stations and planktonic size fractions (60–2000 µm) ranged from +0.05 to +1.23‰ and was isotopically heavier than the particulate fraction (-0.03 to +0.54‰; 0.8-51 µm; Little et al., 2018) and marine aerosols (+0.00 to +0.18‰; Little et al., 2014) measured in the South Atlantic. The Zn isotopic composition

($\delta^{66}Zn$) in the different stations and planktonic size fractions (60–2000 µm) was relatively narrower, varying from +0.33 to +0.59‰. It was also isotopically heavier than $\delta^{66}Zn$ measured in marine particles of the central Atlantic Ocean (+0.15 to +0.43‰; Maréchal et al., 2000). It should be noticed that the MERITE-HIPPOCAMPE campaign was conducted in spring and, an increase of $\delta^{66}Zn$ values was already observed during bloom events in oceanic waters (Maréchal et al., 1998) as well as in lacustrine systems (Peel et al., 2009). A general examination of data did not allow to identify any clear trend between $\delta^{65}Cu$ and $\delta^{66}Zn$ and their respective concentrations (Cu and Zn), neither as a function of spatial distribution, nor as a function of size fractions (Fig. S1 as supplementary information).

The distribution of trace metal in planktonic food web is driven by complex biogeochemical cycles (Collier and Edmond, 1984; Bruland and Lohan, 2003; Sunda, 2012). As micronutrients, Cu and Zn are essential to phytoplankton activities through photosynthesis processes and construction of macromolecules (Morel et al., 2008). Then, trace metal are transferred into the trophic food web through dietary pathway (Sun et al., 2020). Besides biological processes, geogenic particles issued from rivers, effluents and atmospheric deposition (Radakovich et al., 2008; Oursel et al., 2013) may contribute to the $\delta^{65}Cu$ and $\delta^{66}Zn$ signatures found in plankton. Hence, the $\delta^{65}Cu$ and $\delta^{66}Zn$ fingerprint observed here in the different planktonic size fractions may result from both biological/trophic transfer processes and geogenic inputs, the discrimination between the two remaining technically challenging (Cullen and Sherrell, 1999; Cloquet et al., 2008; Plaquette and Sherrell, 2012; Baconnais et al., 2019).

3.2. Geogenic contribution on Cu and Zn isotopic compositions in plankton

Geogenic particles (*i.e.* minerals from natural and anthropogenic sources) are ubiquitous and enter in marine ecosystems through various processes such as weathering, atmospheric

deposition, sediment resuspension (Bianchi, 2007). The variations of $\delta^{65}Cu$ and $\delta^{66}Zn$ in geogenic particles are greater than 1‰ and encompass multiple natural and anthropogenic sources (Fig. 3). For example, in the natural soil, due to the large variability of geological zones, $\delta^{65}Cu$ and $\delta^{66}Zn$ vary widely from -0.15 to +0.44‰ and from -0.03 to +0.43‰, respectively (Fekiacova et al., 2015). Similar variations are also found in Saharan dusts ($\delta^{65}Cu$ = -0.01 ± 0.14‰ and $\delta^{66}Zn$ = +0.19 ± 0.15‰; Schleicher et al., 2020) or marine particles ($\delta^{65}Cu$ = +0.23 ± 0.20‰; Little et al., 2018 and $\delta^{66}Zn$ = +0.35 ± 0.08‰; Maréchal et al., 2002). Based on a compilation of results from basaltic and ultramafic samples from different geological zones, the isotopic fingerprint of Cu and Zn in a bulk silicate earth (BSE) can be estimated as $\delta^{65}Cu$ = +0.06 ± 0.20‰ and $\delta^{66}Zn$ = +0.28 ± 0.05‰ (Chen et al., 2013; Liu et al., 2015). However, establishing a natural baseline seems difficult to achieve because similar $\delta^{65}Cu$ and $\delta^{66}Zn$ can also be found in other natural particles such as carbonates ($\delta^{66}Zn$ = +0.73 ± 0.41‰; Fekiacova et al., 2015), Fe-Mn nodules ($\delta^{65}Cu$ = +0.31 ± 0.23‰ and $\delta^{66}Zn$ = +0.90 ± 0.28‰; Maréchal et al., 2000), chalcopyrite ($\delta^{65}Cu$ = -1.91 ± 2.50‰; Mathur et al., 2005; 2014) and sphalerite ($\delta^{66}Zn$ = +0.17 ± 0.20‰; Sonke et al., 2008).

The artificial anthropogenic processes, such as ore refining and electrolysis, can also fractionate isotopes leading to fingerprints in byproducts distinguishable from natural background. Redox processes can induce Cu isotopic fractionation, whereby Cu^{II}-bound products are enriched in heavier isotopes while Cu^{I}-bound products are preferentially composed of lighter isotopes (Ehrlich et al., 2004). As a result, major $\delta^{65}Cu$ variations in anthropogenic reservoirs can be found in pesticides (from -0.49 to +0.89‰; Blotevogel et al., 2018), antifouling paints (Briant et al., 2022), urban aerosol (Souto-Oliviera et al., 2018; 2019) and in traffic-related inputs (from -0.18 to +0.71‰ with a median value of +0.34‰; Dong et al., 2017). Due to its low boiling point temperature and high fractionation in evaporation–condensation processes, Zn isotopic fractionation varies widely in coal activities (-0.10 to +1.35‰; Desaulty

et al., 2020). In addition to contamination from fossil combustion, industrial activities also release Zn particles. For example, δ^{66}Zn varies from +0.5 to +1.3‰ in metallurgic and electroplating waste (Sirvy et al., 2008; Araújo et al., 2017), from -0.1 to +0.6‰ in non-exhaust traffic emission (Dong et al., 2017), from +0.11 to +0.71‰ in galvanized hardware (John et al., 2007b), from +0.38 to +0.76‰ near Pb-Zn smelter (Juillot et al., 2011), from +0.40 to +0.46‰ in ZnO fumes (Shield et al., 2010), and from +0.18 to +0.20‰ in N-fertilizer or +0.40 to +0.44‰ in P-fertilizer (Chen et al., 2008).

To assess the potential influence of geogenic particles on Cu and Zn isotopic compositions of Mediterranean plankton, δ^{65}Cu and δ^{66}Zn variations were examined in relation to Cu/POP and Zn/POP in the four size fractions, according to the three geographical zones (Fig. 4). Two pools of samples stand out. The first pool (Pool 1) was composed of samples with great δ^{65}Cu and δ^{66}Zn variations (from +0.05 to +1.23‰ and from +0.33 to +0.59‰, respectively) in relation to low Cu/POP and Zn/POP ratios (from 1.1 to 3.4 µg/mg and from 20.9 to 44.9 µg/mg, respectively). The second pool (Pool 2) was composed of samples with lower δ^{65}Cu and δ^{66}Zn variations (from +0.29 to +0.59‰ and from +0.35 to +0.48‰, respectively) in relation to higher Cu/POP and Zn/POP ratios (from 5.9 to 8.7 µg/mg and from 63.6 to 100.7 µg/mg, respectively).

According to our companion paper (Chifflet et al., 2022), samples from Pool 2 seemed dominated by a geogenic component since they samples were poor in organic matter with a biotic component < 40%. Otherwise, the samples from Pool 1 were organic rich with a biotic component ranging from 60 to 100% (Table 2). The Ti is known to be a geogenic element (Ohnemus and Lam, 2015) unaffected by biological uptake or particulate recycling (Dammshäuser et al., 2013). Therefore, Ti/POP ratio can be used to represent geogenic *vs* biotic particles. While the Cu/POP *vs* Ti/POP diagram showed clear relationships with samples from the same geographic area, these trends appeared more nuanced with the Zn diagram (Fig. 5).

Due to geographic characteristics (distance from shore, bathymetry), waters from the northern and southern coastal zones were very likely more influenced by weathering processes and sediment resuspension than were waters from the offshore zone. The increase of Cu/POP and Ti/POP ratios were concomitant to the relative decrease of the biotic compartment against the geogenic counterpart. The two linear trends observed in the Cu diagram probably represented a 'geogenic-dilution' line of the northern and southern coastal zones. Slopes suggest different geogenic sources and outpoints (*e.g.* St1-F6, St2-F3, St4-F5, St17-F4) could be due to poor separation of plankton size fractions in the field. The offshore values overlap the lower end of the 'geogenic-dilution' lines, showing a mixture of geogenic particles in both the northern and southern coastal zones. Different anthropogenic source contributions could explain the different slopes and the isotopic fingerprint overlapping. Therefore, Cu and Zn geogenic sources could not be identified precisely in our samples. On-board particle sieving could not be as selective as expected and geogenic particles may have remained "stuck" or accumulated with some fractions when washing was not performed optimally.

3.3. Effects of the trophic transfer and homeostasis on Cu and Zn isotopic compositions

Cu and Zn isotopic compositions increased with $\delta^{15}N$, indicating an enrichment in heavy isotopes in the higher trophic levels (Fig. 6). Only samples from the southern coastal zone did not follow this pattern. The trophic Cu and Zn isotope fractionation has been already studied in mammals from terrestrial and marine environments (Jaouen et al., 2013; Araújo et al., 2021), but isotope patterns in marine food webs remain unknown so far. Despite this gap, it is recognized that speciation, uptake mechanisms and metabolism are key parameters controlling trophic isotope fractionation in plankton-zooplankton realm.

Cu and Zn are essential elements involved in many metabolic mechanisms making it difficult to identify the main biological mechanisms driving their isotopic fractionation in the

frame of field studies. Indeed, each metabolic pathway (adsorption, precipitation, redox) can induce isotopic fractionation in favor of one isotope or another. For example, Cu uptake into a biofilm can cause a relative enrichment of ^{65}Cu and Cu uptake across the cell membrane can favor ^{63}Cu (Bigalke et al., 2010; Courtaud et al., 2014). Furthermore, the enzymatic activity involved in Cu^{I}-Cu^{II} redox processes modifies the Cu fractionation with Cu^{I} species in favor of light isotope (Zhu et al., 2002; Ehrlich et al., 2004; Navarrete et al., 2011; Fujii et al., 2013; Moynier et al., 2017). Similar to Cu, biological processes can also be invoked to explain Zn isotopic composition in the planktonic food web. Previously, ^{66}Zn enrichment in planktonic biomass was found to vary from +0.19 and +0.43‰ depending on species and environmental conditions (Maréchal et al., 2000; Gélabert et al. 2006; John et al. 2007a). In natural environment, the main processes inducing Zn fractionation are adsorption (with organic or inorganic ligands) and diffusion (Cloquet et la., 2008; Coutaud et al., 2014). While Zn adsorption on organic matter and carrier proteins are mechanisms of heavy isotope enrichment in marine organisms (Weiss et al., 2005; Gélabert et al., 2006; John and Conway, 2014), diffusion of Zn through the phytoplanktonic cell is preferentially into lighter Zn (John et al., 2007a; Peel et al., 2009; John and Conway, 2014).

During the MERITE-HIPPOCAMPE campaign, samples from four size fractions were subsampled for bacterial (Quéméneur et al., 2022), phytoplanktonic (Bellaaj Zouari et al., 2022) and zooplanktonic (Fierro-González et al., 2022) diversity, taxonomy and abundance. Hence, Spearman correlations between $\delta^{65}Cu$ and $\delta^{66}Zn$ values and abundances of various bacteria, phytoplankton and zooplankton species were investigated (Table S1 as supplementary information). When considering all stations, significant ($p < 0.05$) but weak correlations ($r < 0.5$) were found for all parameters. However, some discrepancies were observed at regional scale. In the northern coastal zone, $\delta^{66}Zn$ was strongly correlated with the relative abundance of the phylum *Firmicutes* ($r = 0.81$, $p < 0.05$) (Table S2 as supplementary information), which

includes heterotrophic bacteria usually present during decomposition processes in water and sediments (Zhao et al., 2017). In the offshore zone, δ^{65}Cu was strongly correlated with *Prochlorococcus sp*., the phylum *Cyanobacteria* and picoeukaryotes ($r = 0.78$, $p < 0.05$) (Table S3 as supplementary information). In the southern coastal zone, while δ^{65}Cu and δ^{66}Zn were moderately correlated with *Firmicutes* ($r = -0.66$ and 0.57, $p < 0.05$, respectively), δ^{65}Cu was strongly correlated with zooplanktonic organisms, i.e., copepods ($r = -0.94$, $p < 0.05$) (Table S4 as supplementary information).

Under strong anthropogenic pressure, coastal waters receive both large inputs of nutrients that can stimulate phytoplanktonic activities (Cruzado and Velasquez, 1990; Macias et al., 2019) and a cocktail of contaminants that can induce changes in the biodiversity of primary producers (Hulot et al., 2000; Johnston and Roberts, 2009; Goni-Urriza et al., 2018). In such conditions, Cu can reduce copepods eggs production, thus negatively impact primary predator communities (Lauer and Bianchini, 2010). Furthermore, bacteria are known to strongly fractionate Cu ($\Delta^{65}Cu_{media\text{-}cell}$ from +1.0 to +4.4‰; Navarrete et al., 2010), and lower interactions between bacteria and phytoplankton were already observed by Pringault et al. (2020; 2021) in contaminated Bizerte Lagoon (southeastern Mediterranean Sea, Tunisia). The lower δ^{65}Cu values in the southern coastal zones and the strong anti-correlation with copepods could suggest a discrepancy in the southern coastal zone. The impact of Cu in the Gulf of Gabès (southern coastal zone) should be further investigated as a significant transfer of Cu into the planktonic food web was also observed in a companion study (Chifflet et al., 2022).

4. Conclusions

In this study, we propose an isotopic approach to examine the Cu and Zn transfers in the planktonic food web in three geographical areas of the Mediterranean Sea: the northern

coastal zone (bays of Toulon and Marseille, France), the offshore zone (near the Balearic Thermal Front) and the southern coastal zone (Gulf of Gabès, Tunisia). Overall, geogenic particles were ubiquitous in the different sizes of plankton (60–200, 200–500, 500–1000, 1000–2000 µm) and the Cu and Zn isotope compositions seems to reflect a complex mixing of signatures of geogenic (from natural and anthropic sources) and planktonic assemblages. Nevertheless, elemental and isotope Cu-Zn data combined with proxies for geogenic (Ti) and organic matter (POP) indicated that geogenic particles in the northern and southern coastal zone were of different origins, and that in the offshore, geogenic particles were from a mixture of northern and southern sources. The δ^{65}Cu and δ^{66}Zn variations were examined in relation to δ^{15}N and showed trends of heavy isotope enrichment in the planktonic food web from the northern and offshore zones. Discrepancies were observed between the southern coastal zone and the latter two zones. While δ^{65}Cu was strongly correlated with *Prochlorococcus sp*. and picoeukaryotes in the offshore zone, δ^{65}Cu was strongly correlated with copepods in the southern coastal zone. We suggest that the southern coastal zone exhibits a shift in the community structure due to Cu biogeochemical interactions. Furthermore, the bacterial phylum *Firmicutes* was found correlated with δ^{66}Zn, suggesting decomposition of particulate matter at the DCM in Mediterranean coastal ecosystems.

In the framework of the MERITE-HIPPOCAMPE campaign, a companion study showed amplification of essential and non-essential elements (As, Cu, Cr, Sb) in biotic compartment of southern coastal zones (Chifflet et al., 2022). The present study confirms the impact of trace metal on planktonic food web of the Mediterranean Sea. During the campaign, we encountered challenging weather conditions with winds up to 40 knots and 3 m waves. As a result, collecting and sieving particles on-board was operationally difficult without time for replicates. For future research, we recommend limiting studies to homogeneous geographic

areas (same physico-chemical characteristics of waters, same anthropogenic influences) and collecting plankton in size fractions ranging from 0.2 to 2000 µm.

Authors contribution. All the authors participated in the MERITE-HIPPOCAMPE project and contributed to the sampling strategy, preparation of the material, field work, laboratory analyses and/or data processing and interpretation. SC and NB wrote the original manuscript, and all the authors participated to its reviewing and/or editing.

Acknowledgments. The MERITE-HIPPOCAMPE project was initiated and funded by the "Pollution & Contaminants" transversal axis of the CNRS-INSU MISTRALS program (joint action of the MERMEX-MERITE and CHARMEX subprograms). It has also received the financial support of the Franco-Tunisian International Joint Laboratory (LMI) COSYS-Med. The MERITE-HIPPOCAMPE campaign was organized and supported by the French (Oceanographic Fleet, CNRS/INSU, IFREMER, IRD) and Tunisian institutions (Ministry of Agriculture, Hydraulic Resources and Fisheries of Tunisia, Ministry of Higher Education and Scientific Research of Tunisia). The project has also received additional funding from the MIO's incentive "Action Sud" and "Transverse" programs (CONTAM project) and by the ANR CONTAMPUMP (ANR JCJC #19-CE34-0001-01). We acknowledge the MIO's platforms: "Service Atmosphère-Mer" (SAM) for the preparation and management of the embarked material and, "Plateforme Analytique de Chimie des Environnements Marins" (PACEM), the staff from LBCM-Ifremer laboratory for various chemical analyses and the staff from AETE-ISO platform from the OSU-OREME university for the MC-ICP-MS analyses.

The authors are deeply grateful for the thorough and constructive corrections and insightful comments of the anonymous reviewers, who have significantly improved the original manuscript.

References

Araújo, D.F., Boaventura, G.R., Viers, J., Mulholland, D.S., Weiss, D., Araújo, D., Lima, B., Ruiz, I., Machado, W., Babinski, M., Dantas, E., 2017. Ion exchange chromatography and mass bias correction for accurate and precise Zn isotope ratio measurements in environmental reference materials by MC-ICP-MS. J. Braz. Chem. Soc., 28, 225–235.

Araújo, D.F., Ponzevera, E., Briant, N., Knoery, J., Bruzac, S., Sireau, T., Grouhel-Pellouin, A., Brach-Papa, C., 2021. Differences in Copper Isotope Fractionation Between Mussels (Regulators) and Oysters (Hyperaccumulators): Insights from a Ten-Year Biomonitoring Study. Environ. Sci. Technol., 55, 324-330.

Araújo, D.F., Knoery, J., Briant, N., Vigier, N., Ponzevera, E., 2022a. "Non-traditional" stable isotopes applied to the study of trace metal contaminants in anthropized marine environments. Mar. Pollut. Bull., 175, 113398.

Araújo, D.F., Knoery, J., Briant, N., Ponzevera, E., Mulholland, D.S., Bruzac, S., Sireau, T., Chouvelon, T., 2022b. Cu and Zn stable isotopes in suspended particulate matter sub-fractions from the northern Bay of Biscay help identify biogenic and geogenic particle pools. Cont. Shelf Res., 244, 104791.

Archer, C., Andersen, M.B., Cloquet, C., Conway, T.M., Dong, S., Ellwood, M., Moore, R., Nelson, J., Rehkämper, M., Rouxel, O., Samanta, M., Shin, K.-C., Sohrin, Y., Takano, S.,

Wasylenki, L., 2017. Inter-calibration of a proposed new primary reference standard AA-ETH Zn for zinc isotopic analysis. J. Anal. At. Spectrom. 32, 415–419.

Baconnais, I., Rouxel, O., Dulaquais, G., Boye, M., 2019. Determination of the copper isotope composition of seawater revisited: a case study from the Mediterranean Sea. Chem. Geol., 511, 465-480.

Bellaaj Zouari, A., et al., 2022. Analysis of phytoplankton and bacterioplakton variations and structure along a North-south Mediterranean transect. Mar. Pollut. Bull., in prep in this special issue.

Bianchi, C.N., Morri, C. 2000. Marine biodiversity of the Mediterranean Sea: situation, problems and prospects for future research. Mar. Pollut. Bull., 40, 367-376.

Bianchi, T.S., 2007. Biogeochemistry of estuaries. Oxford University Press.

Bigalke, M., Weyer, S., Wilcke, W., 2010. Copper Isotope Fractionation during Complexation with Insolubilized Humic Acid. Environ. Sci. Technol., 44, 5496-5502.

Blotevogel, S., Oliva, P., Sobanska, S., Viers, J., Vezin, H., Audry, S., Prunier, J., Darrozes, J., Orgogozo, L., Courjault-Radé, P., Schreck, E., 2018. The fate of Cu pesticides in vineyard soils: a case study using δ^{65}Cu isotopes ratios and EPR analysis. Chem. Geol., 477, 35-46.

Borrok, D.M., Wanty, R.B., Ridley, W.I., Wolf, R., Lamothe, P.J., Adams, M., 2007. Separation of copper, iron, and zinc from complex aqueous solutions for isotopic measurement. Chem. Geol., 242, 400-414.

Briant, N., Freydier, R., Araújo, D., Delpoux, S., Elbaz-Poulichet, F., 2022. Cu isotope records of Cu-based antifouling paints in sediment core profiles from the largest European Marina, The Port Camargue. Sci. Tot. Environ., 157885.

Bruland, K.W., Lohan, M.C., 2003. Control of trace metals in seawater. Treatise Geom., 6, 23-47.

Chen, J., Gaillardet, J., Louvat, P., 2008. Zinc isotopes in the Seine River waters, France: a probe of anthropogenic contamination. Environ. Sci. Technol., 42, 6494-6501.

Chen, H., Savage, P.S., Teng, F.-Z., Helz, R.T., Moynier, F., 2013. Zinc isotope fractionation during magmatic differentiation and the isotopic composition of the bulk earth. Earth Planet. Sci. Lett., 369-370, 34-42.

Chifflet, S., Briant, N., Tesán-Onrubia, J.A., Zaaboub, N., Armi, S., Radakovitch, O., Bănaru, D., Tedetti, M., 2022. Distribution and accumulation of metals and metalloids in the planktonic food web of the Mediterranean Sea (MERITE-HIPPOCAMPE campaign). Mar. Pollut. Bul., 185, accepted.

Chouvelon, T., Strady, E., Harmelin-Vivien, M, Radakovitch, O., Brach-Papa, C., Crochet, S., Knoery, J., Rozuel, E., Thomas, B., Tronczynski, J., Chiffoleau, J.F., 2019. Patterns of trace metal bioaccumulation and trophic transfer in a phytoplankton-zooplankton-small pelagic fish marine food web. Mar. Pollut. Bull., 146, 1013-1030.

Cloquet, C., Carignan, J, Lehmann, M.F., Vanhaecke, F., 2008. Variation in the isotopic composition of zinc in the natural environment and the use of zinc isotopes in biogeosciences: a review. Anal. Bioanal. Chem, 390, 451-463.

Coale, K.H., Bruland, K.W., 1988. Copper complexation in the Northeast Pacific. Limnol. Oceanogr., 33, 1084-1101.

Coll, M., Albo-Puigserver, M., Navarro J., Palomera, I., Dambacher, J.M., 2019. Who is to blame? Plausible pressures on small pelagic fish population changes in the northwestern Mediterranean Sea. Mar. Ecol. Prog. Ser., 617-618, 277-294.

Collier, R., Edmond, J., 1984. The trace element geochemistry in marine biogenic particulate matter. Progr. Oceanogr., 13, 113-199.

Conway, T.M., John, S.G., 2014. The biogeochemical cycling of zinc and zinc isotopes in the North Atlantic Ocean. Glob. Biogeochem. cycles, 28, 1111-1124.

Conway, T.M., Horner, T.J., Plancherel, Y., González, A.G., 2021. A decade of progress in understanding cycles of trace elements and their isotopes in the oceans. Chem. Geol., 580, 120381.

Coutaud, A., Meheut, M., Viers, J., Rols, J.-L., Pokrovsky, O. S., 2014. Zn isotope fractionation during interaction with phototrophic biofilm. Chem. Geol., 390, 46-60.

Cox, A., Saito, M.A., 2013. Proteomic responses of oceanic *Synechococcus* WH8102 to phosphate and zinc scarcity and cadmium additions. Front. Microbiol., 4, article 387.

Criss, R., 1999. Principle of stable isotope distribution. Oxford University Press, Oxford

Croot, P.L., Moffett, J.W., Brand, L.E., 2000. Production of extracellular Cu complexing ligands by eukaryotic phytoplankton in response to Cu stress. Limnol. Oceanogr., 45, 619-627.

Cruzado, A., Velasquez, Z.R., 1990. Nutrients and phytoplankton in the Gulf of Lions, northwestern Mediterranean. Cont. Shelf Res., 9-11, 931-942.

Cullen, J., Sherrell, R.M., 1999. Techniques for determination of trace metals in small samples of size-fractionated particulate matter: Phytoplankton metals off central California. Mar. Chem., 67, 233-247.

Dammshäuser, A., Wagener, T., Garbe-Schönberg, D., Croot, P., 2013. Particulate and dissolved aluminum and titanium in the upper water column of the Atlantic Ocean. Deep-Sea Res. I, 73(C), 127-139.

Desaulty, A.M., Petelet-Giraud, EM., 2020. Zinc isotope composition as a tool for tracing sources and fate of metal contaminants in rivers. Sci. Tot. Environ., 728, 138599.

Desboeufs, K., Fu, F., Bressac, M., Tovar-Sánchez, A., Triquet, S., Doussin, J.-F., Giorio, C., Chazette, P., Disnaquet, J., Feron, A., Formenti, P., Maisonneuve, F., Rodríguez-Romero, A., Zapf, P., Dulac, F., Guieu, C., 2022. Wet deposition in the remote western and central

Mediterranean as a source of trace metals to surface seawater. Atmospheric Chemistry and Physics, 22, 2309–2332, https://doi.org/10.5194/acp-22-2309-2022.

Domsic, J.F., Avvaru, B.S., Kim, C.H., Gruner, S.M., Agbandje-McKenna, M., Silverman, D.N., McKenna, R., 2008. Entrapment of Carbon Dioxide in the Active Site of Carbonic Anhydrase II. J. Biol. Chem., 283, 30766-30771.

Dong, S., Ochoa Gonzalez, R., Harrison, R.M., Green, D., North, R., Fowler, G., Weiss, D., 2017. Isotopic signatures suggest important contributions from recycled gasoline, road dust and non-exhaust traffic sources for copper, zinc and lead in PM10 in London, United Kingdom. Atmos. Environ., 165, 88-98.

Druce, M., Stirling, C.H., Rolinson, J.M., 2020. High-precision zinc isotopic measurement of certified reference materials relevant to the environmental, earth, planetary and biomedical sciences. Geostand. Geoanalytical Res., 44, 711-732.

Ehrlich, S., Butler, I., Halicz, L., Rickard, D., Oldroyd, A., Matthews, A., 2004. Experimental study of the copper isotope fractionation between aqueous Cu(II) and covellite, CuS. Chem. Geol., 209, 259-269.

Fekiacova, Z., Cornu, S., Pichat, S., 2015. Tracing contamination sources in soils with Cu and Zn isotopic ratios. Sci. Total Environ., 517, 96-105.

Fierro-González, P., Pagano, M., Guilloux, L., Makhlouf, N., Tedetti, M., Carlotti F. 2022. Zooplankton biomass, size structure, and associated metabolic fluxes with focus on its roles at the chlorophyll maximum layer during the plankton-contaminant MERITE-HIPPOCAMPE cruise. Mar. Pollut. Bul., submitted to this special issue.

Fujii, T., Moynier, F., Abe, M., Nemoto, K., Albarède, F., 2013. Copper isotope fractionation between aqueous compounds relevant to low temperature geochemistry and biology. Geochim. Cosmochim. Acta, 110, 29-44.

Gélabert, A., Pokrovsky, O.S., Viers, J., Schott, J., Boudou, A., Feurtet-Mazel, A., 2006. Interaction between zinc and freshwater and marine diatom species: surface complexation and Zn isotope fractionation. Geochim. Cosmochim. Acta, 70, 839-857.

Goni-Urriza, M., Moussard, H., Lafabrie, C., Carre, C., Bouvy, M., Sakka Hlaili, A., Pringault, O., 2018. Consequences of contamination on the interactions between phytoplankton and bacterioplankton. Chemosphere, 195, 212-222.

Graham, S., Pearson, N., Jackson, S., Griffin, W., O'Reilly, S.Y., 2004. Tracing Cu and Fe from source to porphyry: in situ determination of Cu and Fe isotope ratios in sulfides from the Grasberg Cu–Au deposit. Chem. Geol., 207, 147-169.

Guieu, C., Loÿe-Pilot, M.D., Ridame, C., Thomas C. 2002. Chemical characterization of the Saharan dust end-member: Some biogeochemical implications for the western Mediterranean Sea, J. Geophys. Res., 107 (D15), 4258

Heimbürger, L.E., Mignon, C., Dufour, A., Chiffoleau, J.F., Cossa, D., 2010. Trace metal concentrations in the North-western Mediterranean atmospheric aerosol between 1986 and 2008: Seasonal patterns and decadal trends. Sci. Tot. Environ., 408, 2629-2638.

Heimbürger, L.E., Mignon, C., Cossa, D., 2011. Impact of atmospheric deposition of anthropogenic and natural trace metals on Northwestern Mediterranean surface waters: A box model assessment. Environ. Pollut., 159, 1629-1634.

Ho, T.Y., Wen, L.S., You, C.F., Lee, D.C., 2007. The trace metal composition of size-fractionated plankton in the South China Sea: Biotic versus abiotic sources. Limnol. Oceanogr., 52, 1776-1788.

Hulot, F.D., Lacroix, G., Lescher-Moutoue, F.O., Loreau, M., 2000. Functional diversity governs ecosystem response to nutrient enrichment. Nature, 405, 340-344.

Jaouen, K., Pons, M.L., Balter, V., 2013. Iron, copper and zinc isotopic fractionation up mammal trophic chains. Earth Planet. Sci. Lett., 374, 164-172.

Jeandel, C., Rutgers van der Loeff, M., Lam, P.J., Roy-Barman, M., Sherrell, R.M., Kretschmer, S., German, C., Dehairs, F., 2015. What did we learn about ocean particle dynamics in the GEOSECS–JGOFS era? Progr. Oceanogr., 133, 6-16.

John, S. G., Conway, T.M., 2014. A role for scavenging in the marine biogeochemical cycling of zinc and zinc isotopes. Earth Planet. Sci. Lett., 394, 159-167.

John, S.G., Geis, R.W., Saito, M.A., Boyle, E.A., 2007a. Zinc isotope fractionation during high affinity and low-affinity zinc transport by the marine diatom Thalassiosira oceanica. Limnol. Oceanogr., 52, 2710-2714.

John, S. G., Genevieve Park, J., Zhang, Z., Boyle, E. A., 2007b. The isotopic composition of some common forms of anthropogenic zinc. Chem. Geol., 245, 61–69.

Johnston, E.L., Roberts, D.A., 2009. Contaminants reduce the richness and evenness of marine communities: a review and meta-analysis. Environ. Pollut., 157, 1745-1752.

Juillot, F., Maréchal, C., Morin, G., Jouvin, D., Cacaly, S., Telouk, P., Benedetti, M.F., Ildefonse, P., Sutton, S., Guyot, F., Brown, G.E. Jr, 2011. Contrasting isotopic signatures between anthropogenic and geogenic Zn and evidence for post depositional fractionation processes in smelter-impacted soils from Northern France. Geochim. Cosmochim. Acta, 75, 2295-2305.

Lacoste, E., Raimbault, P., Harmelin-Vivien, M., Gaertner-Mazouni, N., 2016. Trophic relationships between the farmed pearl oyster *Pinctada margaritifera* and its epibionts revealed by stable isotopes and feeding experiments. Aquacult. Environ. Interact., 8, 55-66.

Larson, P.B., Maher, K., Ramos, F.C., Chang, Z., Gaspar, M., Meinert, L., 2003. Copper isotope ratios in magmatic and hydrothermal ore-forming environments. Chem. Geol., 201, 337-350.

Lauer, M.M., Bianchini, A., 2010. Chronic copper toxicity in the estuarine copepod *Acartia Tonsa* at different salinities. Environ. Toxicol. Chem., 29, 2297-2303.

Lam, P.J., Lee, J.M., Heller, M.I., Mehic, S., Xiang, Y., Bates, N.R., 2018. Size-fractionated distributions of suspended particle concentration and major phase composition from the U.S. GEOTRACES Eastern Pacific Zonal Transect (GP16). Mar. Chem., 201, 90-107.

Lemaitre, N., de Souza, G.F., Archer, C., Wang, R.M., Planquette, H., Sarthou, G., Vance, D., 2020a. Pervasive sources of isotopically light zinc in the North Atlantic Ocean. Earth Planet. Sci. Lett., 539, 116216.

Liao, W.H., Yang, S.C., Ho, T.Y., 2017. Trace metal composition of size-fractionated plankton in the Western Philippine Sea: The impact of anthropogenic aerosol deposition. Limnol. Oceanogr., 62, 2243-2259.

Little, S.H., Vance, D., Walker-Brown, C., Landing, W.M., 2014. The oceanic mass balance of copper and zinc isotopes, investigated by analysis of their inputs, and outputs to ferromanganese oxide sediments. Geochim. Cosmochim. Acta, 125, 673-693.

Little, S.H., Archer, C., Milne, A., Schlosser, C., Achterberg, E.P., Lohan, M.C., Vance, D., 2018. Paired dissolved and particulate phase Cu isotope distributions in the South Atlantic. Chem. Geol., 502, 29-43.

Liu, S.A., Huang, J., Liu, J., Wörner, G., Yang, W., Tang, Y.J., Chen, Y., Tang, L., Zheng, J., Li, S., 2015. Copper isotopic composition of the silicate Earth. Earth Planet. Sci. Lett., 427, 95-103.

Llamas-Dios, M.I., Vadillo, I., Jimenez-Gavilan, P., Candela, L., Corada-Fernandez, C., 2021. Assessment of a wide array of contaminants of emerging concern in a Mediterranean water basin (Guadalhorce river, Spain): Motivations for an improvement of water management and pollutants surveillance. Science of the Total Environment, 788, 147822.

Luy, N., Gobert, S., Sartoretto, S., Biondo, R., Bouquegneau, J.M., Richir, J., 2012. Chemical contamination along the Mediterranean French coast using *Posidonia oceanica* (L.) Delile above-ground tissues: a multiple trace element study. Ecol. Indic., 18, 269-277.

Macias, D., Huertas, I.E., Garcia-Gorriz, E., Stips, A., 2019. Non-Redfieldian dynamics driven by phytoplankton phosphate frugality explain nutrient and chlorophyll patterns in model simulations for the Mediterranean Sea. Progr. Oceanogr., 173, 37-50.

Maher, K.C., Larson, P.B., 2007. Variation in copper isotope ratios and controls on fractionation in hypogene skarn mineralization at Coroccohuayco and Tintaya, Peru: copper isotope ratios in magmatic and hydrothermal ore-forming environments. Econ. Geol., 102, 225-237.

Marañón, E., Wambeke, F., Uitz, J., Boss, E., Dimier, C., Dinasquet, J., Engel, A., Haëntjens, N., Pérez-Lorenzo, M., Taillandier, V., Zäncker, B., 2021. Deep maxima of phytoplankton biomass, primary production and bacterial production in the Mediterranean Sea. Biogeosciences, 18, 1749-1767.

Maréchal, C.N., 1998. Géochimie isotopique du cuivre et du zinc : méthode, variabilité naturelle et application océanographique. Thèse Univ J. Fourier, Grenoble I (France), 260pp.

Maréchal, C.N., Telouk, P., Albarède, F., 1999. Precise analysis of copper and zinc isotopic composition by plasma-source mass spectrometry. Chem. Geol., 156, 251-273.

Maréchal, C.N., Nicolas, E., Douchet, C., Albarède, F., 2000. Abundance of zinc isotopes as a marine biogeochemical tracer. Geochem. Geophys., 1, 1-15.

Maréchal, C., Abrarède, F., 2002. Ion-exchange fractionation of copper and zinc isotopes. Geochim. Cosmochim. Acta, 66, 1499-1509.

Mason, T.F.D., Weiss, D.J., Chapman, J.B., Wilkinson, J.J., Tessalina, S.G., Spiro, B., Horstwood, M.S.A., Spratt, J., Coles, B.J., 2005. Zn and Cu isotopic variability in the Alexandrinka volcanic-hosted massive sulphide (VHMS) ore deposit, Urals, Russia. Chem Geol., 221, 170-187.

Mathur, R., Ruiz, J., Titley, S., Liermann, L., Buss, H., Brantley, S., 2005. Cu isotopic fractionation in the supergene environment with and without bacteria. Geochim. Cosmochim. Acta, 69, 5233-5246.

Mathur, R., Munk, L.A., Townley, B., Gou, K.Y., Gómez Miguélez, N., Titley, S., Chen, G.G., Song, S., Reich, M., Tornos, F., Ruiz, J., 2014. Tracing low-temperature aqueous metal migration in meniralized watersheds with Cu isotope fractionation. Appl. Geochem., 51, 109-115.

The MerMex Group, 2011. Marine ecosystems' responses to climatic and anthropogenic forcings in the Mediterranean. Progress in Oceanography, 91, 97-166.

Micheli, F., Halpern, B.S., Walbridge, S., Ciriaco, S., Ferretti, F., Fraschetti, S., Lewison, R., Nykjaer, L., Rosenberg, A.A., 2013. Cumulative Human Impacts on Mediterranean and Black Sea Marine Ecosystems: Assessing Current Pressures and Opportunities. PLOS One, 8, e79889.

Moffett, J.W., Zika, R.G., Brand, L.E., 1990. Distribution and potential sources and sink of copper chelators in the Sargasso Sea. Deep Sea Res. (A), 37, 27-36.

Moffett, J.W., Brand, L.E., 1996. Production of strong, extracellular Cu chelators by marine cyanobacteria in response to Cu stress. Limnol. Oceanogr., 41, 388-395.

Moffett, J.W., Brand, L.E., Croot, P.L., Barbeau, K.A., 1997. Cu speciation and cyanobacterial distribution in harbors subject to anthropogenic Cu inputs. Limnol Oceanogr., 42, 789-799.

Morel, M.M., Price, N.M., 2003. Biogeochemical cycles of trace metals in the oceans. Science, 300, 944-947.

Morel, F.M.M., 2008. The co-evolution of phytoplankton and trace element cycles in the oceans. Geobiol., 6, 318-324.

Moynier, F., Vance, D., Fujii, T., Savage, P., 2017. The Isotope Geochemistry of Zinc and Copper. Rev. Mineral. Geochem., 82, 543-600.

Navarrete, J., Borrok, D., Viveros, M., Ellzey, J., 2011. Copper isotope fractionation during surface adsorption and intracellular incorporation by bacteria. Geochim. Cosmochim. Acta, 75, 784-799.

Ohnemus, D., Lam, P.J., 2015. Cycling of lithogenic marine particles in the US GEOTRACES North Atlantic transect. Deep-Sea Res. II, 116, 283-302.

Oursel, B., Garnier, C., Durrieu, G., Mounier, S., Omanović, D., Lucas, Y., 2013. Dynamics and fates of trace metals chronically input in a Mediterranean coastal zone impacted by a large urban zone. Mar. Pollut. Bull., 69, 137-149.

Peel, K., Weiss, D., Sigg, L., 2009. Zinc isotope composition of settling particles as a proxy for biogeochemical processes in lakes: Insights from the eutrophic Lake Greifen, Switzerland, Limnol. Oceanogr., 54, 1699-1708.

Peers, G., Quesnel, S.A., Price, N.M., 2005. Copper requirements for iron acquisition and growth of coastal and oceanic diatoms. Limnol. Oceanogr., 50, 1149-1158.

Peers, G., Price, N. M., 2006. Copper-containing plastocyanin used for electron transport by an oceanic diatom. Nature, 441, 341-344.

Petit, J.C.J., de Long, J., Chou, L., Mattielli, N., 2008. Development of Cu and Zn isotope MC-ICP-MS measurements: application to suspended particulate matter and sediments from the Scheldt estuary. Geostand. Geoanalytical Res., 32, 149-166.

Pey, J., Pérez, N., Querol, X., Alastuey, A., Cusack, M., Reche, C., 2010. Intense winter atmospheric pollution episodes affecting the Western Mediterranean. Sci. Tot. Environ., 408, 1951-1959.

Planquette, H., Sherrell, R.M., 2012. Sampling for particulate trace element determination using water sampling bottles: methodology and comparison to in situ pumps. Limnol. Oceanogr. Methods, 10, 367-388.

Pringault, O., Bouvy, M., Carre, C., Fouilland, E., Meddeb, M., Mejri, K., Leboulanger, C., Hlaili, A.S., Sakka Hlaili, A., 2020. Impacts of chemical contamination on bacterio-phytoplankton coupling. Chemosphere, 257, 127165.

Pringault, O., Bouvy, M., Carre, C., Mejri, K., Bancon-Montigny, C., Gonzalez, C., Leboulanger, C., Hlaili, A.S., Goni-Urriza, M., 2021. Chemical contamination alters the interactions between bacteria and phytoplankton. Chemosphere, 278, 130457.

Quéméneur, M., Lajnef, R., Cabrol, L., Mission, B., Tedetti, M., Chifflet, S., Belhassen, M., Bellaj Zouari, A., 2022. Prokaryotic diversity within various size-fractions of plankton and associated contaminants along a North-South Mediterranean transect. Mar. Pollut. Bull., in prep in this special issue.

Radakovich, O., Roussiez, V., Ollivier, P., Ludwig, W., Grenz, C., Probst, J.L., 2008. Particulate heavy metals input from rivers and associated sedimentary deposits on the Gulf of Lion continental shelf. Estuar. Coast. Shelf Sci., 77, 285-295.

Raimbault P., Garcia, N., 2008. Evidence for efficient regenerated production and dinitrogen fixation in nitrogen-deficient waters of the South Pacific Ocean: impact on new and export production estimates. Biogeosciences, 5, 323-338.

Rouxel, O., Fouquet, Y., Ludden, J.N., 2004. Copper Isotope Systematics of the Lucky Strike, Rainbow, and Logatchev Sea-Floor Hydrothermal Fields on the Mid-Atlantic Ridge. Chem. Geol., 99, 585-600.

Rossi, N., Jamet, J.L., 2008. In situ heavy metals (copper, lead and cadmium) in different plankton compartments and suspended particulate matter in two coupled Mediterranean coastal ecosystems (Toulon bay, France). Mar. Pollut. Bull., 56, 1862-1870.

Rue, E., Bruland, K., 2001. Domoic acid binds iron and copper: a possible role for the toxin produced by the marine diatom Pseudo-nitzschia. Mar. Chem., 76, 127-134.

Ryan, B.M., Kirby, J.K., Degryse, F., Scheiderich, K., McLaughlin, M.J., 2014. Copper isotope fractionation during equilibration with natural and synthetic ligands. Environ. Sci. Technol., 48, 8620-8626.

Schleicher, N., Dong, S., Packman, H., Little, S.H., Ochoa Gonzales R., Najorka, J., Sun, Y., Weiss, D.J., 2020. A global assessment of copper, zinc and lead isotopes in mineral dust sources and aerosols. Front. Earth Sci., 8, 167.

Shaked, Y., Xu, Y., Leblanc, K., Morel, M.M., 2006. Zinc availability and alkaline phosphatase activity in Emiliania huxleyi: Implications for Zn-P co-limitation in the ocean. Limnol. Oceanogr., 51, 299-309.

Shield, A.E., Weis, D., Orians, K.J., 2010. Evaluation of zinc, cadmium and lead isotope fractionation during smelting and refining. Sci. Tot. Environ., 408, 2357-2368.

Sivry, Y., Riotte, J., Sonke, J.E., Audry, S., Schäfer, J., Viers, J., Blanc, G., R. Freydier, R., . Dupré B., 2008. Zn isotopes as tracers of anthropogenic pollution from Zn-ore smelters The Riou Mort–Lot River system. Chem. Geol., 255, 295-304.

Sonke, J.E., Sivry, Y., Viers, J., Freydier, R., Dejonghe, L., André, L., Aggarwal, J.K., Fontan, F., Dupré, B., 2008. Historical variations in the isotopic composition of atmospheric zinc deposition from a zinc smelter. Chem. Geol., 252, 145-157

Souto-Oliviera, C.E., Babinski, M., Araújo, D., Andrade, M.F., 2018. Multi-isotopic fingerprints (Pb, Zn, Cu) applied for urban aerosol source apportionment and discrimination. Sci. Tot. Environ., 626, 1350-1366.

Souto-Oliviera, C.E., Babinski, M., Araújo, D., Weiss, D.J., Ruiz, I.R., 2019. Multi-isotope approach of Pb, Cu and Zn in urban aerosols and anthropogenic sources improves tracing of the atmospheric pollutant sources in megacities. Atmos. Environ., 198, 427-437.

Sunda, W., 2012. Feedback interactions between trace metal nutrients and phytoplankton in the ocean. Front. Microbiol., 3, 204.

Takano, S., Liao, W.H., Tian, H.A., Huang, K.F., Ho, T.Y., Sohrin, Y., 2020. Source of particulate Ni and Cu in the water column of the northern South China Sea: evidence from elemental and isotope ratios in aerosols and sinking particles. Mar. Chem., 219, 103751.

Tedetti, M., Tronczynski, J., 2019. HIPPOCAMPE cruise, RV Antea. https://doi.org/10.17600/18000900

Tedetti, M., Tronczynski, J., Carlotti, F., Pagano, M., Sammari, C., Bel Hassen, M., Ben Ismail, S., Desboeufs, K., Poindron, C., Chifflet, S., Abdennadher, M., Amri, S., Bănarua, D., Ben Abdallah, L., Bhairy, N., Boudriga, I., Bourin, A., Brach-Papa, C., Briant, N., Cabrol, L., Chevalier, C., Chouba, L., Coudray, S., Daly Yahia, M.N., de Garidel-Thoroni T., Dufour, A., Dutay, J.-C., Espinasse, B., Fierro, P., Fornier, M., Garcia, N., Giner, F., Guigue, C., Guilloux, L., Hamza, A., Heimbürger-Boavida, L.-E., Jacquet, S., Knoery, J., Lajnef, R., Makhlouf Belkahia, N., Malengros, D., Martinot, P.L., Bosse, A., Mazur, J.-C., Meddeb, M., Misson, B., Pringault, O., Quéméneur, M., Radakovitch, O., Raimbault, P., Ravel, C., Rossi, V., Rwawi, C., Sakka Hlaili, A., Tesán Onrubia, J.A., Thomas, B., Thyssen, M., Zaaboub, N., Zouari, A., Garnier, C., 2022. Contamination of planktonic food webs in the Mediterranean Sea: Setting the frame for MERITE-HIPPOCAMPE oceanographic cruise (spring 2019). Mar. Pollut. Bull., submitted to this special issue.

Tesán Onrubia, J.A., Tedetti, M., Carlotti, F., Tenaille, M., Guilloux, L., Pagano, M., Lebreton, B., Guillou, G., Fierro-Gonzalez, P., Guigue, C., Chifflet, S., Garcia, T., Boudriga, I., Belhassen, M., Zouari, A., Bănaru, D. Spatial variations of stable isotope ratios and biochemical content of size-fractionated plankton in the Mediterranean Sea (MERITE-HIPPOCAMPE campaign). Mar. Pollut. Bull., submitted to this special issue.

UNEP/MAP-RAC-SPA, 2008. Impact of climate change on biodiversity in the Mediterranean Sea. In: Perez T., RAC/SPA (Eds.), Tunis, 1-61.

Wiederhold, J.G., 2015. Metal stable isotope signatures as tracers in environmental geochemistry. Environ. Sci. Technol., 49, 2606-2624.

Yang, S.C., Hawco, N.J., Pinedo-Gonzales, P., Bian, X., Huang, K.F., Zhang, R., John, S.G., 2020. A new purification method for Ni and Cu stable isotopes in seawater provides evidence for widespread Ni isotope fractionation by phytoplankton in the North Pacific. Chem. Geol., 547, 119662.

Zhao, Y., Vance, D., Abouchami, W., de Baar, H.J.W., 2014. Biogeochemical cycling of zinc and its isotopes in the Southern Ocean. Geochim. Cosmochim. Acta, 125, 653-672.

Zhao, D., Cao, X., Huang, R., Zeng, J., Wu, Q.L., 2017. Variation of bacterial communities in water and sediments during the decomposition of *Microcystis* biomass. Plos One, 12, e0176397.

Zhu, X. K., Guo, Y., Williams, R. J. P., O'nions, R. K., Matthews, A., Belshaw, N. S., Salvato, B., 2002. Mass fractionation processes of transition metal isotopes. Earth Planet. Sci. Lett., 200, 47-62.

Zumft, W.G., Kroneck, P.M.H., 2007. Respiratory transformation of nitrous oxide (N_2O) to dinitrogen by Bacteria and Archaea. Adv. Microb. Physiol., 52, 107-225.

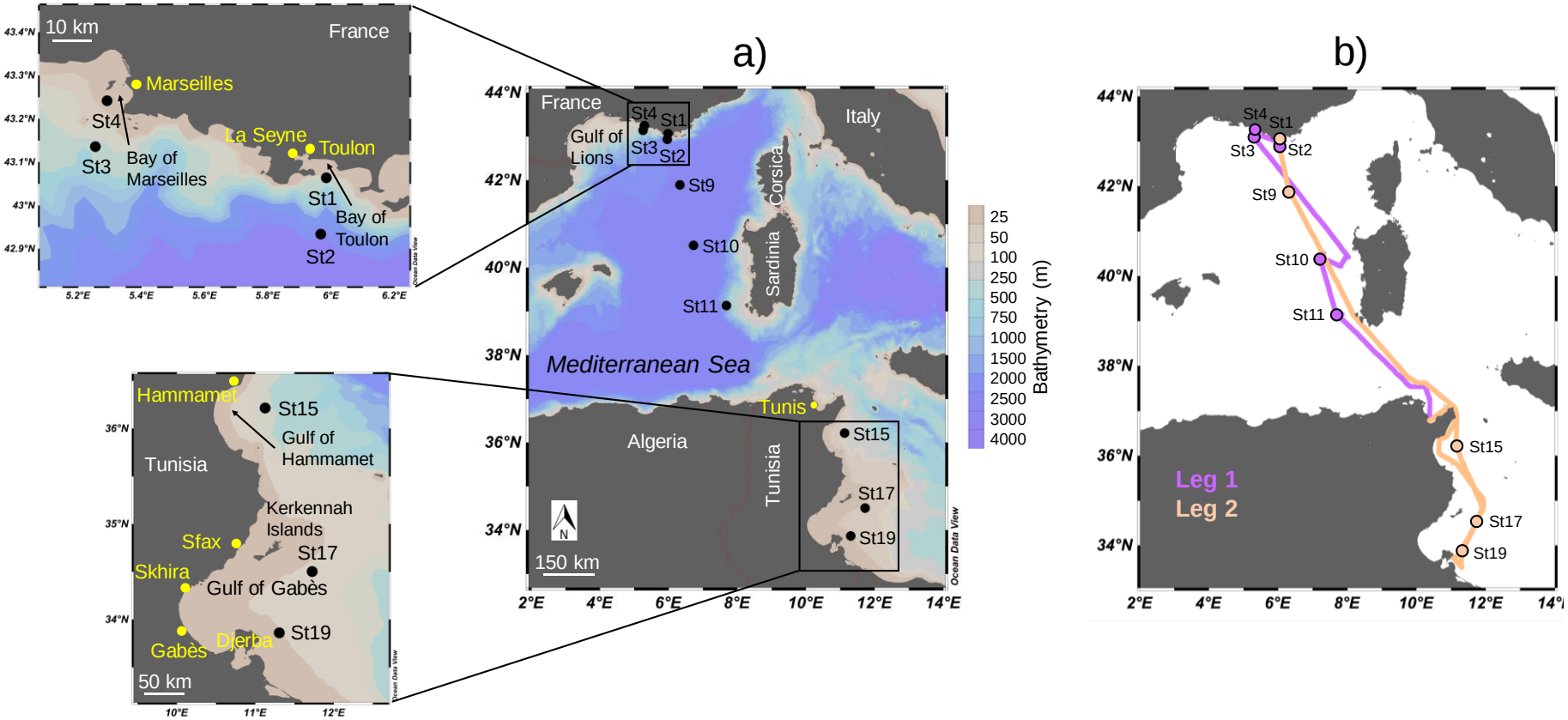

Figure 1. a) Location of the sampling stations in the Mediterranean Sea. b) Details of the MERITE-HIPPOCAMPE campaign tracks: Leg 1 (from La Seyne-sur-Mer to Tunis) with five sampling stations (St2, St4, St3, S10 and St11, in this chronological order); Leg 2 (from Tunis to Gulf of Gabès to La Seyne-sur-Mer) with five sampling stations (St15, St17, St19, St9 and St1, in this chronological order).

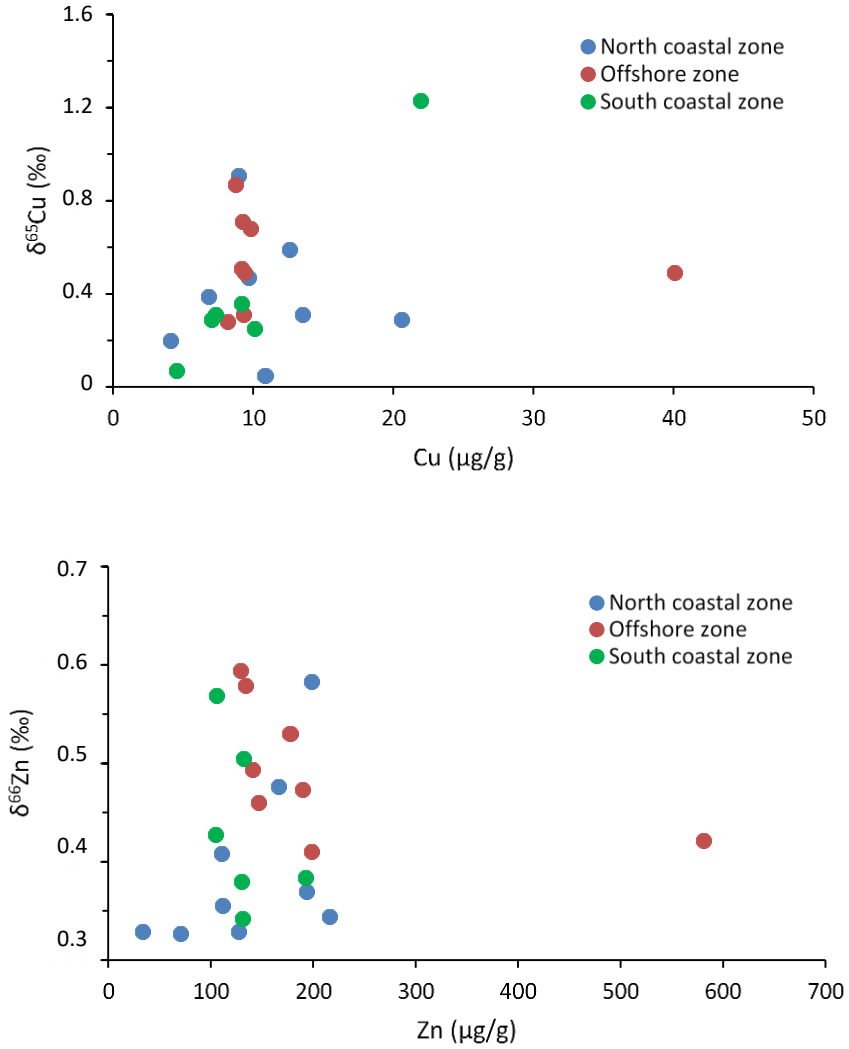

Figure 2. $\delta^{65}Cu$ and $\delta^{66}Zn$ variations relative to Cu and Zn concentrations in the four size fractions plankton (F3: 60–200, F4: 200–500, F5: 500–1000 and F6: 1000–2000 µm), respectively. Isotopic compositions are in ‰ and concentrations in µg/g of dry sample. Values are grouped according to three geographical zones: the northern coastal zone (blue), the offshore zone (red) and the southern coastal zone (green).

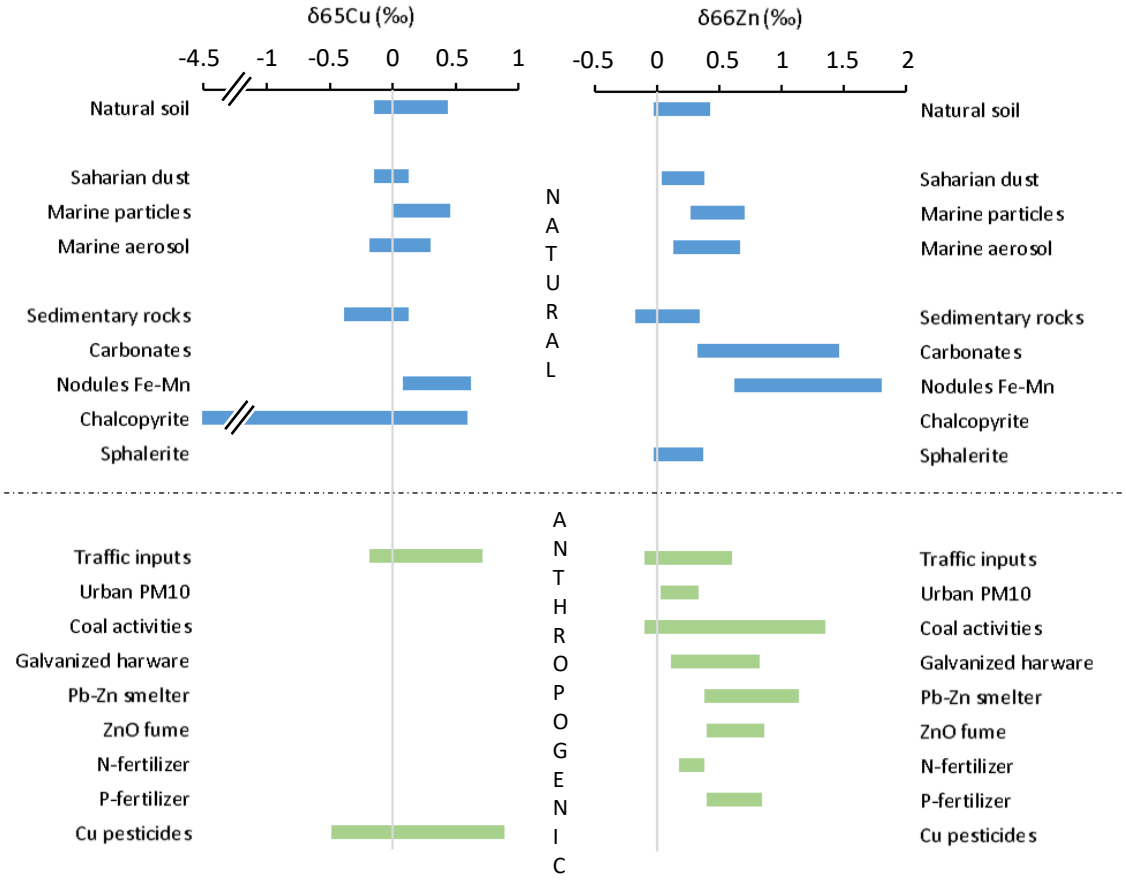

Figure 3. Summary of various $\delta^{65}Cu$ and $\delta^{66}Zn$ compositions in geogenic (natural and anthropogenic) sources.

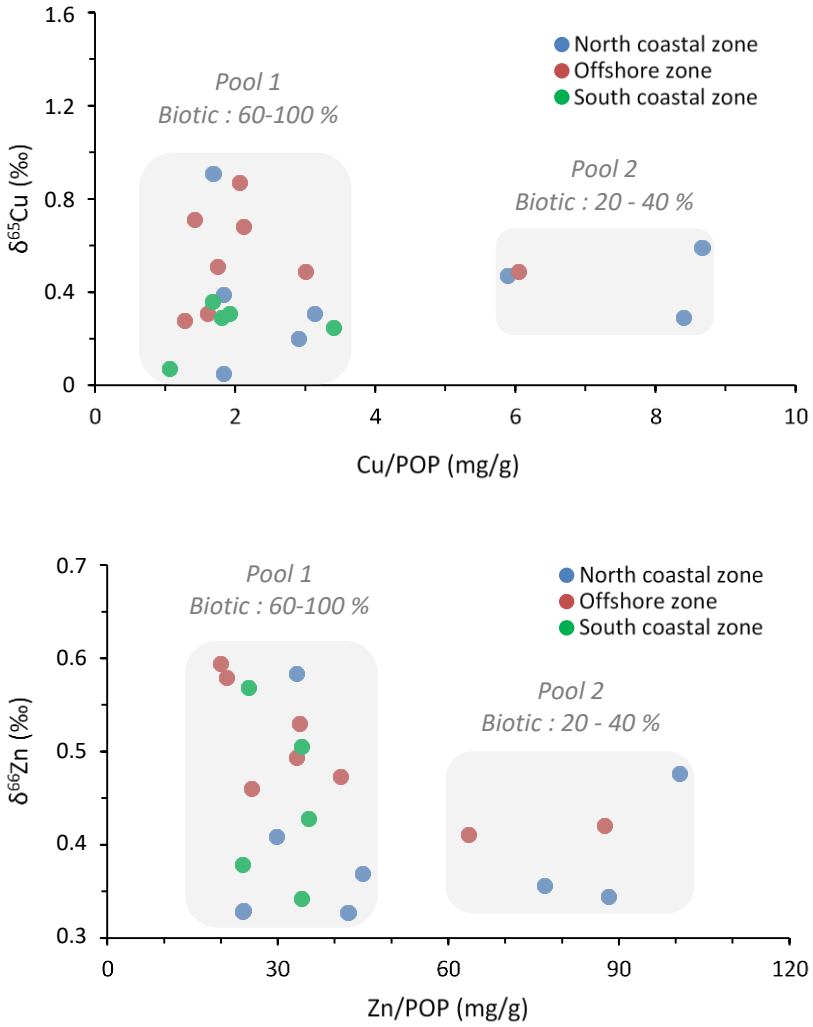

Figure 4. δ^{65}Cu and δ^{66}Zn variations relative to their corresponding Cu/POP and Zn/POP ratios in the four size fractions plankton (F3: 60–200, F4: 200–500, F5: 500–1000 and F6: 1000–2000 µm). Values are grouped according to three geographical zones: the northern coastal zone (blue), the offshore zone (red) and the southern coastal zone (green).

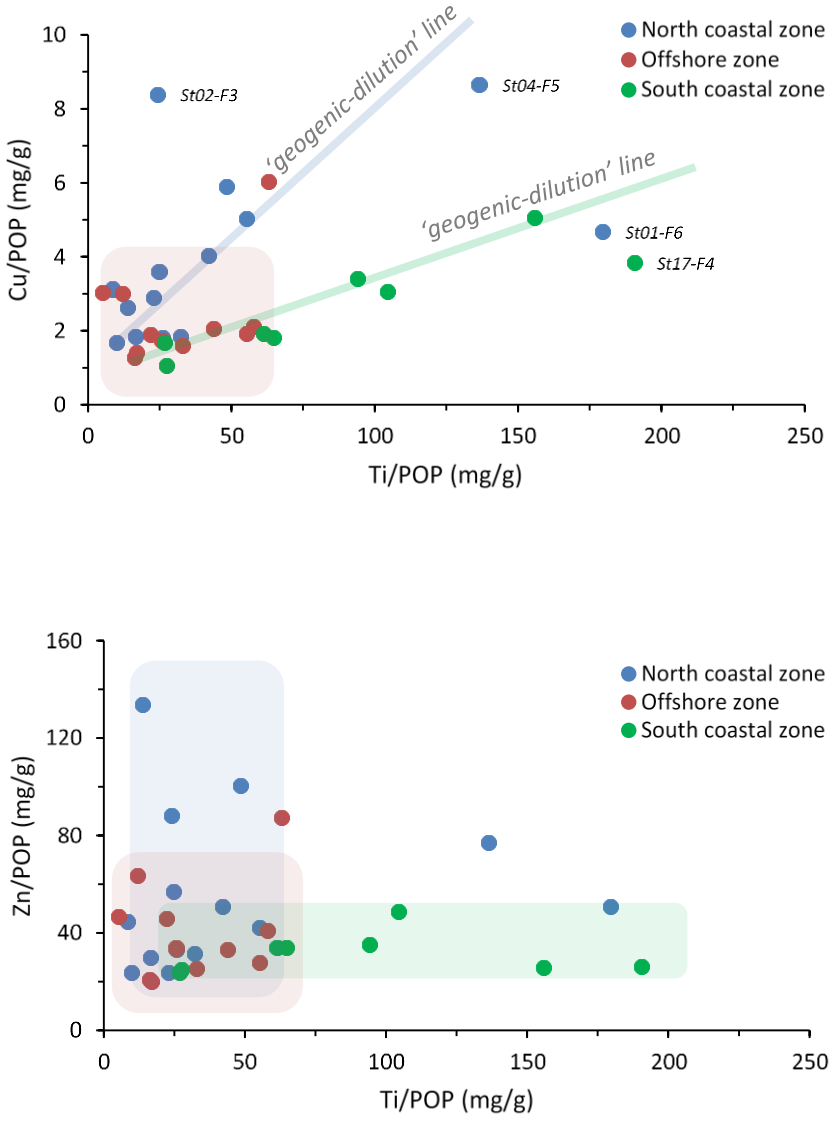

Figure 5. Cu/POP vs Ti/POP and Zn/POP vs Ti/POP diagrams in the four size fractions plankton (F3: 60–200, F4: 200–500, F5: 500–1000 and F6: 1000–2000 µm). Values are grouped according to three geographical zones: the northern coastal zone (blue), the offshore zone (red) and the southern coastal zone (green).

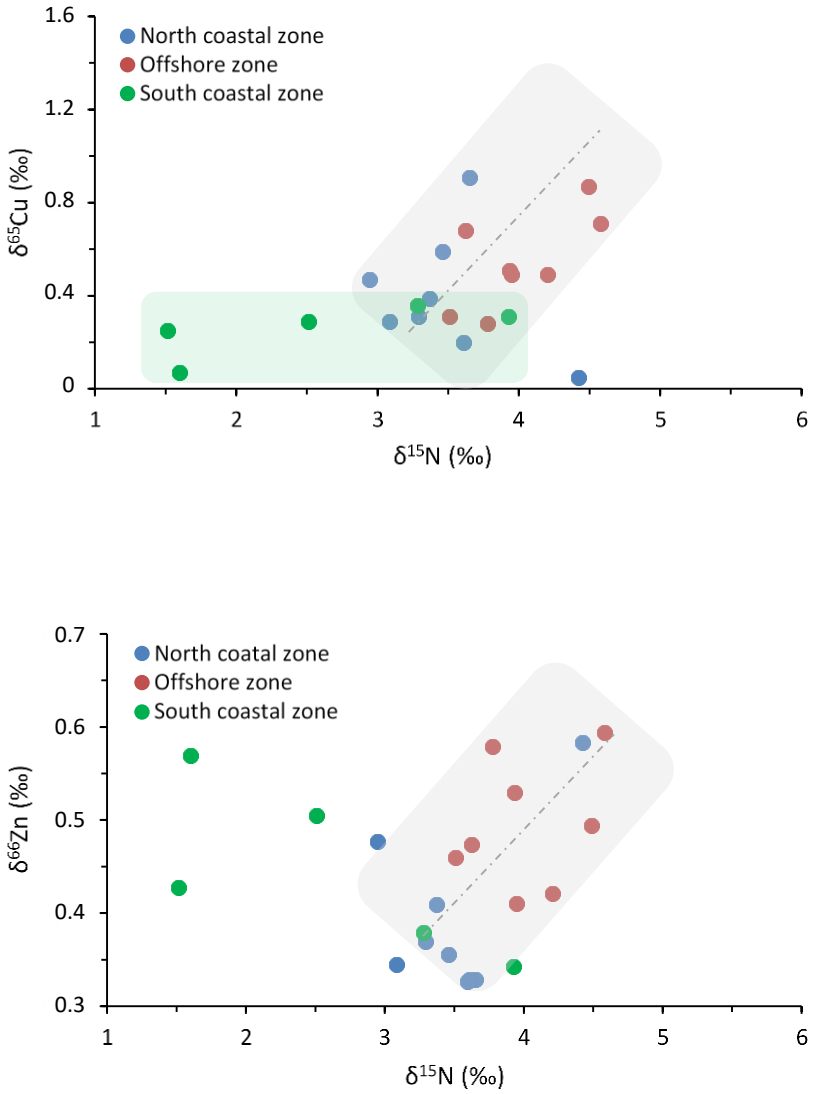

Figure 6. $\delta^{65}Cu$ and $\delta^{66}Zn$ variations relative to their corresponding $\delta^{15}N$ in the four size fractions plankton (F3: 60–200, F4: 200–500, F5: 500–1000 and F6: 1000–2000 µm). Isotopic compositions are in ‰. Values are grouped according to three geographical zones: the northern coastal zone (blue), the offshore zone (red) and the southern coastal zone (green).

Table 1. General information about the 10 stations sampled during the MERITE-HIPPOCAMPE campaign (April 13-May 14, 2019) aboard the *R/V Antea*.

Station	Latitude (N)	Longitude (E)	Localisation	Depth (m)	DCM (m)	Characteristics
St1	43°03.819'	5°59.080'	Toulon	91	20	Urbanized bay; intermittently bloom area
St2	42°56.020'	5°58.041'	Toulon	1770	25	Limit of continental shelf; intermittently bloom area
St3	43°08.150'	5°15.280'	Marseilles	95	55	Southeast entrance to the Gulf of Lions; intermittently bloom area
St4	43°14.500'	5°17.500'	Marseilles	58	31	Urbanized bay; intermittently bloom area
St9	41°53.508'	6°19.998'	Offshore	2575	20	North of the Balearic Thermal Front; Bloom area
St10	40°18.632'	7°14.753'	Offshore	2791	50	South of the Balearic Thermal Front; intermittently bloom area
St11	39°07.998'	7°41.010'	Offshore	1378	40	Algerian ecoregion; no bloom area
St15	36°12.883'	11°07.641'	Gulf of Hammamet	100	66	Near Sicily channel; No bloom area and high density of small pelagic fishes
St17	34°30.113'	11°43.573'	Gulf of Gabes	48	40	Gabès ecoregion; coastal bloom area, high density of small pelagic fishes
St19	33°51.659'	11°18.509'	Gulf of Gabes	50	40	Gabès ecoregion; coastal bloom area, high density of small pelagic fishes

Table 2. Multiparametric values obtained during the MERITE HIPPOCAMPE campaign (spring 2019) in the four planktonic size fractions (F3: 60-200 µm; F4: 200-500 µm; F5: 500-1000 µm; F6: 1000-2000 µm) and the 10 stations (St1-4, St9-11, St15, St17, St19). Details of trace metal (Ti, µg/g), particulate organic phosphorus (POP, mg/g) and biotic component (Biotic, %) were presented in Chifflet et al (2022) and, details of nitrogen isotopic compositions ($\delta^{15}N$, ‰) were presented in Tésan-Onrubia et al. (2022) as companion papers.

Station	Fraction	Biotic (%)	Ti (µg/g)	POP (mg/g)	$\delta^{15}N$ (‰)
Northern coastal zone (Marseilles-Toulon bays)					
St01	F3	68	150.3	4.67	3.20
St01	F4	83	52.7	5.32	3.65
St01	F5	67	153.9	5.94	4.42
St01	F6	35	445.1	2.48	4.26
St02	F3	43	59.1	2.45	3.09
St02	F4	98	36.7	4.31	3.29
St02	F5	81	93.6	3.78	3.48
St02	F6	81	132.6	3.16	3.52
St03	F3	30	79.5	1.64	2.94
St03	F4	42	54.8	3.97	3.39
St03	F5	93	61.6	3.71	3.37
St03	F6	-	-	3.17	3.34
St04	F3	70	32.3	1.40	3.61
St04	F4	40	91.9	1.67	3.60
St04	F5	22	197.6	1.45	3.46
St04	F6	-	243.1	-	-
Offshore zone (near the Balearic Thermal Front and the Algerian ecoregion)					
St09	F3	100	59.4	2.70	1.99
St09	F4	98	16.5	3.19	2.73
St09	F5	90	37.6	3.11	3.95
St09	F6	-	37.8	-	-
St10	F3	74	267.0	4.61	3.62
St10	F4	90	133.9	5.24	3.94
St10	F5	84	186.2	4.24	4.49
St10	F6	89	274.7	4.98	5.67
St11	F3	80	191.1	5.80	3.51
St11	F4	89	103.7	6.39	3.78
St11	F5	23	417.4	6.64	4.20
St11	F6	85	110.4	6.48	4.58
Southern coastal zone (Gulf of Gabès)					
St15	F3	66	316.0	3.03	3.56

St15	F4	83	234.9	3.83	3.93
St15	F5	88	146.1	5.47	3.28
St15	F6	-	264.5	-	-
St17	F3	61	178.1	1.14	1.86
St17	F4	64	290.3	1.52	2.41
St17	F5	-	590.4	-	-
St17	F6	-	-	-	-
St19	F3	60	278.6	2.96	1.51
St19	F4	97	116.5	4.26	1.60
St19	F5	-	251.6	3.88	2.51
St19	F6	-	842.9	-	-

Table 3. Concentrations (µg/g) and isotopic compositions (‰) of Cu and Zn in four planktonic size fractions (F3: 60-200 µm; F4: 200-500 µm; F5: 500-1000 µm; F6: 1000-2000 µm) collected at the deep chlorophyll maximum (DCM) according to three geographical areas (the northern coastal zone, the offshore zone, and the southern coastal zone).

Station	Fraction	Cu (µg/g)	Zn (µg/g)	$\delta^{65}Cu$ (‰)	$2\sigma_{Cu}$ (‰)	$\delta^{66}Zn$ (‰)	$2\sigma_{Zn}$ (‰)
Northern coastal zone (Marseilles-Toulon bays)							
St1	F3	8.63	148.10	-	-	-	-
St1	F4	8.95	126.70	0.91	0.02	0.33	0.03
St1	F5	10.85	197.97	0.05	0.01	0.58	0.03
St1	F6	11.60	125.54	-	-	-	-
St2	F3	20.57	216.00	0.29	0.01	0.34	0.03
St2	F4	13.49	193.30	0.31	0.09	0.37	0.03
St2	F5	13.58	214.78	-	-	-	-
St2	F6	12.81	160.32	-	-	-	-
St3	F3	9.69	165.67	0.47	0.01	0.48	0.04
St3	F4	10.42	530.69	-	-	-	-
St3	F5	6.82	110.16	0.39	0.06	0.41	0.03
St3	F6	-	-	-	-	-	-
St4	F3	4.07	33.63	0.2	0.06	0.33	0.03
St4	F4	8.37	70.51	-	-	0.33	0.02
St4	F5	12.55	111.47	0.59	0.01	0.36	0.03
St4	F6	16.99	149.42	-	-	-	-
Offshore zone (near the Balearic Thermal Front and the Algerian ecoregion)							
St9	F3	5.14	124.11	-	-	-	-
St9	F4	9.65	149.54	-	-	-	-
St9	F5	9.36	197.92	0.49	0.03	0.41	0.03
St9	F6	7.50	132.38	-	-	-	-
St10	F3	9.81	189.76	0.68	0.00	0.47	0.04
St10	F4	9.14	177.28	0.51	0.07	0.53	0.04
St10	F5	8.76	141.08	0.87	0.06	0.49	0.04
St10	F6	9.59	139.39	-	-	-	-
St11	F3	9.32	147.16	0.31	0.02	0.46	0.04
St11	F4	8.17	133.56	0.28	0.02	0.58	0.04
St11	F5	40.09	580.68	0.49	0.02	0.42	0.03
St11	F6	9.21	129.32	0.71	0.02	0.59	0.03
Southern coastal zone (Gulf of Gabès)							
St15	F3	9.28	148.03	-	-	-	-
St15	F4	7.33	130.82	0.31	0.02	0.34	0.02
St15	F5	9.14	130.38	0.36	0.01	0.38	0.03

St15	F6	8.18	108.30	-	-	-	-
St17	F3	5.81	29.63	-	-	-	-
St17	F4	5.85	39.70	-	-	-	-
St17	F5	21.92	192.53	1.23	0.01	0.38	0.04
St17	F6	-	-	-	-	-	-
St19	F3	10.08	104.96	0.25	0.05	0.43	0.04
St19	F4	4.52	105.83	0.07	0.01	0.57	0.04
St19	F5	7.02	132.35	0.29	0.01	0.51	0.04
St19	F6	5.62	67.74	-	-	-	-

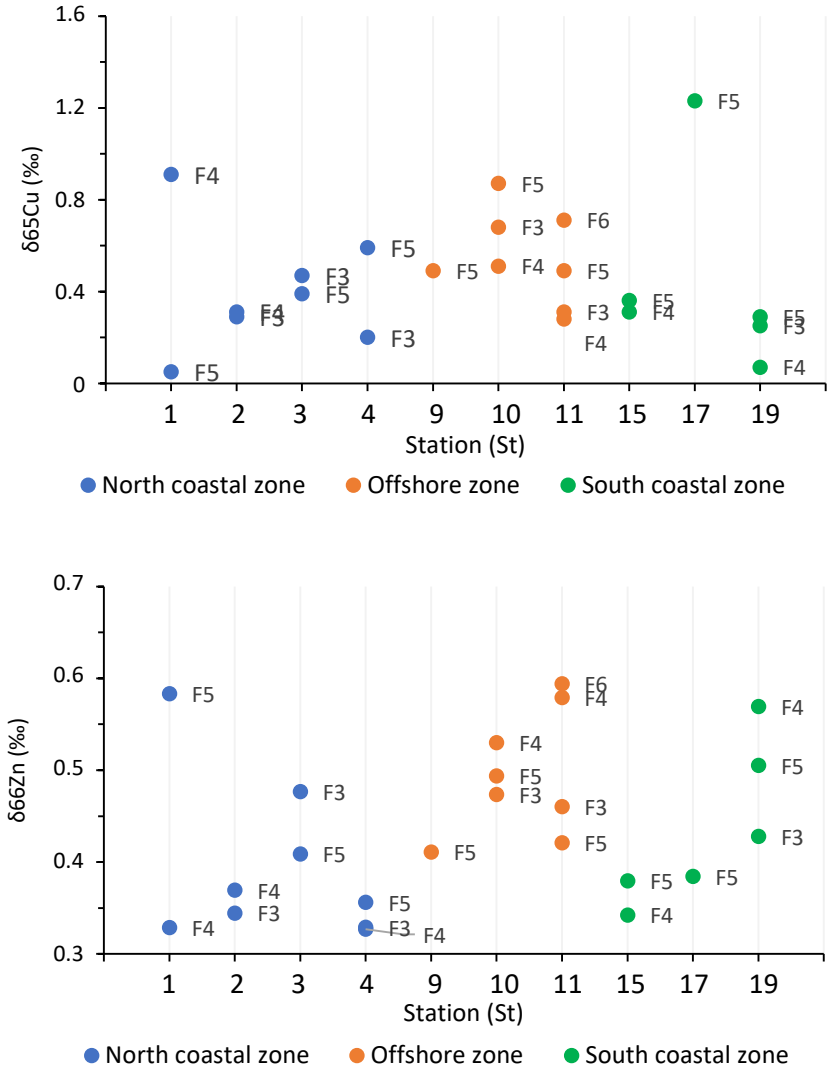

Fig. S1: Histograms showing variations of Cu and Zn isotopic compositions (δ^{65}Cu and δ^{66}Zn) in plankton size fractions (F3: 60–200 µm, F4: 200–500 µm, F5: 500–1000 µm and F6: 1000–2000 µm) per stations (St1-4, St9-11, St15, St17 and St19). Values are colored according to geographical zones: the northern coastal zone (blue), the offshore zone (red) and the southern coastal zone (green).

Table S1: Spearman correlation matrix performed using $\delta^{65}Cu$ and $\delta^{66}Zn$ and the abundance (or relative abundance) of bacterial, phytoplanktonic and zooplanktonic communities in three plankton size fractions (F3: 60–200 µm, F4: 200–500 µm and F5: 500–1000 µm) and the 10 stations (St1-4, St9-11, St15, St17 and St19) with in bold a statistical significance level higher than 95% ($p < 0.05$).

Variables	δ65Cu	δ66Zn	Nanoeukaryotes	Picoeukaryotes	Nauplii	Copepods	*Proteobacteria*	*Cyanobacteria*	*Bacteroidota*	*Actinobacteriota*	*Firmicutes*	*Planctomycetota*	*Verrucomicrobiota*	*Synechococcus*	Cryptophytes	Prokaryotes	*Prochlorococcus*	Crustacea
$\delta^{65}Cu$	**1**																	
$\delta^{66}Zn$	**-0.364**	**1**																
Nanoeukaryotes	**-0.061**	**0.132**	**1**															
Picoeukaryotes	**-0.222**	**0.180**	**-0.510**	**1**														
Nauplii	**-0.190**	-0.001	0.003	**0.505**	**1**													
Copepods	**-0.347**	**0.162**	**0.063**	**0.356**	**0.803**	**1**												
Proteobacteria*	**0.107**	**-0.061**	**0.132**	**0.103**	**-0.036**	**-0.034**	**1**											
Cyanobacteria*	**-0.177**	**0.292**	**-0.207**	**0.221**	**0.136**	**0.029**	**-0.703**	**1**										
Bacteroidota*	**0.126**	**-0.163**	**-0.257**	0.007	**0.057**	-0.003	**-0.572**	**0.171**	**1**									
Actinobacteriota*	**0.185**	**-0.218**	**0.128**	**-0.455**	**-0.412**	**-0.555**	**-0.241**	**0.114**	**0.218**	**1**								
Firmicutes*	**-0.155**	**0.267**	**0.328**	**-0.232**	**-0.189**	**0.063**	**0.145**	**-0.206**	**-0.024**	**-0.274**	**1**							
Planctomycetota*	**-0.446**	**0.109**	**0.131**	**-0.110**	**0.171**	**0.303**	**-0.679**	**0.601**	**-0.043**	**-0.082**	**-0.033**	**1**						
Verrucomicrobiota*	**-0.056**	**0.214**	**-0.159**	**-0.021**	**-0.014**	**0.015**	**-0.741**	**0.638**	**0.563**	-0.001	**0.216**	**0.425**	**1**					
Synechococcus	**-0.110**	**-0.051**	-0.001	**0.472**	**0.186**	**0.055**	**0.722**	**-0.293**	**-0.579**	**-0.416**	**-0.191**	**-0.338**	**-0.658**	**1**				
Cryptophytes	**-0.169**	**-0.019**	**0.200**	**0.445**	**0.554**	**0.459**	**0.121**	**0.085**	**-0.356**	**-0.197**	**-0.405**	**0.140**	**-0.388**	**0.485**	**1**			
Prokaryotes	**0.073**	**-0.287**	**0.128**	**-0.112**	**0.051**	**0.037**	**0.617**	**-0.635**	**-0.497**	**0.126**	**-0.284**	**-0.314**	**-0.807**	**0.396**	**0.352**	**1**		
Prochlorococcus	**0.328**	**0.056**	**-0.166**	**0.172**	**-0.216**	**-0.203**	**0.501**	**-0.264**	**-0.606**	**-0.151**	**-0.299**	**-0.288**	**-0.489**	**0.495**	**0.154**	**0.430**	**1**	
Crustacea	**-0.084**	**-0.029**	**0.236**	**-0.230**	**-0.498**	**-0.403**	**-0.079**	**-0.055**	**0.239**	**0.316**	**0.184**	**-0.144**	**0.093**	**-0.115**	**-0.253**	**-0.301**	**-0.121**	**1**

*Relative abundance of prokaryotic taxa obtained by 16S rRNA gene metabarcoding analysis.

Table S2: Spearman correlation matrix performed using $\delta^{65}Cu$ and $\delta^{66}Zn$ and the abundance (or relative abundance) of bacterial, phytoplanktonic and zooplanktonic communities in three plankton size fractions (F3: 60–200 µm, F4: 200–500 µm and F5: 500–1000 µm) of the northern coastal zone (St1 to St4) with in bold a statistical significance level higher than 95% ($p < 0.05$).

Variables	$\delta^{65}Cu$	$\delta^{66}Zn$	Nanoeukaryotes	Picoeukaryotes	Nauplii	Copepods	*Proteobacteria*	*Cyanobacteria*	*Bacteroidota*	*Actinobacteriota*	*Firmicutes*	*Planctomycetota*	*Verrucomicrobiota*	*Synechococcus*	Cryptophytes	Prokaryotes	*Prochlorococcus*	Crustacea
$\delta^{65}Cu$	**1**																	
$\delta^{66}Zn$	**-0.428**	**1**																
Nanoeukaryotes	**-0.247**	**-0.304**	**1**															
Picoeukaryotes	**0.305**	**0.327**	**-0.988**	**1**														
Nauplii	**0.131**	**-0.541**	**0.758**	**-0.740**	**1**													
Copepods	**0.145**	**-0.552**	**0.514**	**-0.468**	**0.817**	**1**												
Proteobacteria*	**0.329**	**0.350**	**-0.122**	**0.206**	**-0.190**	0.000	**1**											
Cyanobacteria*	**-0.107**	**0.169**	**0.206**	**-0.262**	**0.298**	**-0.064**	**-0.345**	**1**										
Bacteroidota*	**-0.277**	**-0.089**	**-0.122**	**0.094**	**0.183**	**0.135**	**-0.760**	**0.273**	**1**									
Actinobacteriota*	**-0.174**	**-0.034**	**-0.356**	**0.346**	**-0.348**	**-0.200**	**-0.462**	**-0.055**	**0.607**	**1**								
Firmicutes*	0.004	**0.804**	**-0.674**	**0.693**	**-0.657**	**-0.592**	**0.491**	**-0.047**	**-0.149**	**-0.069**	**1**							
Planctomycetota*	**-0.263**	**-0.216**	**0.262**	**-0.271**	**-0.047**	**-0.071**	**-0.273**	**-0.556**	**-0.069**	**-0.113**	**-0.265**	**1**						
Verrucomicrobiota*	**0.085**	**0.132**	**-0.262**	**0.243**	**-0.075**	**-0.235**	**-0.505**	**0.702**	**0.556**	**0.505**	**0.033**	**-0.491**	**1**					
Synechococcus*	**-0.247**	**-0.304**	**1.000**	**-0.988**	**0.758**	**0.514**	**-0.122**	**0.206**	**-0.122**	**-0.356**	**-0.674**	**0.262**	**-0.262**	**1**				
Cryptophytes	**-0.257**	**-0.313**	**0.988**	**-0.964**	**0.767**	**0.569**	**-0.112**	**0.140**	**-0.056**	**-0.262**	**-0.683**	**0.243**	**-0.271**	**0.988**	**1**			
Prokaryotes	**-0.324**	**-0.346**	**0.964**	**-0.952**	**0.758**	**0.578**	**-0.187**	**0.131**	**0.037**	**-0.159**	**-0.711**	**0.234**	**-0.262**	**0.964**	**0.988**	**1**		
Prochlorococcus*	**0.095**	**-0.047**	**0.337**	**-0.205**	**0.351**	**0.523**	**0.300**	**-0.356**	**0.075**	**0.159**	**-0.187**	-0.009	**-0.187**	**0.337**	**0.458**	**0.446**	**1**	
Crustacea	**0.024**	**0.067**	**-0.461**	**0.461**	**-0.463**	**-0.491**	**-0.398**	**-0.095**	**0.334**	**0.429**	**0.048**	**0.191**	**0.445**	**-0.461**	**-0.461**	**-0.461**	**-0.154**	**1**

*Relative abundance of prokaryotic taxa obtained by 16S rRNA gene metabarcoding analysis.

Table S3: Spearman correlation matrix performed using $\delta^{65}Cu$ and $\delta^{66}Zn$ and the abundance (or relative abundance) of bacterial, phytoplanktonic and zooplanktonic communities in three plankton size fractions (F3: 60–200 µm, F4: 200–500 µm and F5: 500–1000 µm) of the offshore zone (St9 to St11) with in bold a statistical significance level higher than 95% ($p < 0.05$).

Variables	$\delta^{65}Cu$	$\delta^{66}Zn$	Nanoeukaryotes	Picoeukaryotes	Nauplii	Copepods	*Proteobacteria*	*Cyanobacteria*	*Bacteroidota*	*Actinobacteriota*	*Firmicutes*	*Planctomycetota*	*Verrucomicrobiota*	*Synechococcus*	Cryptophytes	Prokaryotes	*Prochlorococcus*	Crustacea
$\delta^{65}Cu$	**1**																	
$\delta^{66}Zn$	**0.163**	**1**																
Nanoeukaryotes	**0.499**	**-0.417**	**1**															
Picoeukaryotes	**0.783**	**-0.126**	**0.500**	**1**														
Nauplii	**-0.104**	-0.009	**0.122**	**-0.486**	**1**													
Copepods	**-0.102**	**-0.034**	**0.120**	**-0.478**	**0.983**	**1**												
Proteobacteria*	**0.470**	0.009	**0.315**	**0.234**	**-0.095**	**-0.204**	**1**											
Cyanobacteria*	**-0.296**	**0.026**	**-0.153**	**-0.031**	**0.061**	**0.170**	**-0.930**	**1**										
Bacteroidota*	**-0.157**	**-0.120**	**-0.376**	0.010	**-0.234**	**-0.187**	**-0.461**	**0.183**	**1**									
Actinobacteriota*	0.000	**0.506**	**-0.448**	**0.081**	**-0.701**	**-0.732**	**0.304**	**-0.339**	**0.096**	**1**								
Firmicutes*	**-0.452**	**0.052**	**-0.122**	**-0.794**	**0.632**	**0.579**	**0.217**	**-0.252**	**-0.548**	**-0.235**	**1**							
Planctomycetota*	**-0.470**	**0.266**	**-0.397**	**-0.336**	**0.147**	**0.221**	**-0.739**	**0.843**	**-0.165**	**-0.148**	**0.165**	**1**						
Verrucomicrobiota*	**-0.365**	**-0.077**	**-0.234**	**-0.132**	**0.147**	**0.255**	**-0.983**	**0.948**	**0.426**	**-0.426**	**-0.252**	**0.722**	**1**					
Synechococcus	**0.499**	**-0.417**	**1.000**	**0.500**	**0.122**	**0.120**	**0.315**	**-0.153**	**-0.376**	**-0.448**	**-0.122**	**-0.397**	**-0.234**	**1**				
Cryptophytes	**0.499**	**-0.417**	**1.000**	**0.500**	**0.122**	**0.120**	**0.315**	**-0.153**	**-0.376**	**-0.448**	**-0.122**	**-0.397**	**-0.234**	**1.000**	**1**			
Prokaryotes	**0.499**	**-0.417**	**1.000**	**0.500**	**0.122**	**0.120**	**0.315**	**-0.153**	**-0.376**	**-0.448**	**-0.122**	**-0.397**	**-0.234**	**1.000**	**1.000**	**1**		
Prochlorococcus	**0.783**	**-0.126**	**0.500**	**1.000**	**-0.486**	**-0.478**	**0.234**	**-0.031**	0.010	**0.081**	**-0.794**	**-0.336**	**-0.132**	**0.500**	**0.500**	**0.500**	**1**	
Crustacea	**0.137**	**-0.419**	**0.160**	**0.479**	**-0.816**	**-0.842**	**0.359**	**-0.359**	**0.177**	**0.369**	**-0.450**	**-0.501**	**-0.359**	**0.160**	**0.160**	**0.160**	**0.479**	**1**

*Relative abundance of prokaryotic taxa obtained by 16S rRNA gene metabarcoding analysis.

Table S4: Spearman correlation matrix performed using $\delta^{65}Cu$ and $\delta^{66}Zn$ and the abundance (or relative abundance) of bacterial, phytoplanktonic and zooplanktonic communities in three plankton size fractions (F3: 60–200 µm, F4: 200–500 µm and F5: 500–1000 µm) of the southern coastal zone (St15, St17 and St19) with in bold a statistical significance level higher than 95% ($p < 0.05$).

Variables	$\delta^{65}Cu$	$\delta^{66}Zn$	Nanoeukaryotes	Picoeukaryotes	Nauplii	Copepods	*Proteobacteria*	*Cyanobacteria*	*Bacteroidota*	*Actinobacteriota*	*Firmicutes*	*Planctomycetota*	*Verrucomicrobiota*	*Synechococcus*	Cryptophytes	Prokaryotes	*Prochlorococcus*	Crustacea
$\delta^{65}Cu$	**1**																	
$\delta^{66}Zn$	**-0.745**	**1**																
Nanoeukaryotes	**-0.346**	**0.083**	**1**															
Picoeukaryotes	**-0.238**	**-0.238**	**-0.125**	**1**														
Nauplii	**-0.616**	**0.293**	**0.596**	**0.183**	**1**													
Copepods	**-0.940**	**0.731**	**0.388**	**0.183**	**0.569**	**1**												
Proteobacteria*	**0.327**	**0.073**	**-0.763**	**0.095**	**-0.402**	**-0.235**	**1**											
Cyanobacteria*	**-0.327**	**-0.218**	**0.620**	**0.191**	**0.385**	**0.200**	**-0.945**	**1**										
Bacteroidota*	**-0.118**	**0.100**	**0.763**	**-0.095**	**0.315**	**0.131**	**-0.436**	**0.273**	**1**									
Actinobacteriota*	**0.491**	**-0.418**	**0.286**	**-0.572**	**-0.175**	**-0.601**	**-0.473**	**0.345**	**0.309**	**1**								
Firmicutes*	**-0.664**	**0.573**	**0.405**	**0.191**	**0.542**	**0.844**	0.000	**-0.055**	**0.182**	**-0.709**	**1**							
Planctomycetota*	**-0.527**	**0.200**	**0.334**	**-0.095**	**0.350**	**0.514**	**-0.655**	**0.655**	**-0.255**	**-0.036**	**0.291**	**1**						
Verrucomicrobiota*	**-0.382**	0.018	**0.667**	**-0.191**	**0.489**	**0.392**	**-0.800**	**0.745**	**0.055**	**0.236**	**0.273**	**0.873**	**1**					
Synechococcus	**-0.238**	**-0.238**	**-0.125**	**1.000**	**0.183**	**0.183**	**0.095**	**0.191**	**-0.095**	**-0.572**	**0.191**	**-0.095**	**-0.191**	**1**				
Cryptophytes	**-0.429**	**-0.143**	**0.563**	**0.750**	**0.550**	**0.411**	**-0.429**	**0.572**	**0.429**	**-0.286**	**0.429**	**0.143**	**0.286**	**0.750**	**1**			
Prokaryotes	**0.405**	-0.024	**-0.969**	**-0.125**	**-0.642**	**-0.434**	**0.739**	**-0.667**	**-0.739**	**-0.143**	**-0.453**	**-0.310**	**-0.620**	**-0.125**	**-0.750**	**1**		
Prochlorococcus	**0.346**	**-0.083**	**-1.000**	**0.125**	**-0.596**	**-0.388**	**0.763**	**-0.620**	**-0.763**	**-0.286**	**-0.405**	**-0.334**	**-0.667**	**0.125**	**-0.563**	**0.969**	**1**	
Crustacea	**0.067**	**-0.315**	**0.150**	**0.600**	**-0.220**	**-0.037**	0.000	**0.114**	**0.458**	**-0.114**	0.000	**-0.458**	**-0.343**	**0.600**	**0.600**	**-0.300**	**-0.150**	**1**

*Relative abundance of prokaryotic taxa obtained by 16S rRNA gene metabarcoding analysis.